Micromechanical method for effective piezoelectric properties and electromechanical fields in multi-coated long fiber composites

Georges Chatzigeorgiou, Ali Javili, Fodil Meraghni

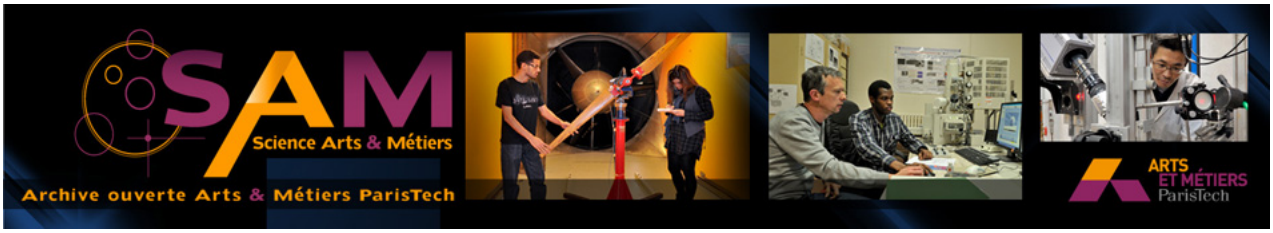

Micromechanical method for effective piezoelectric properties and electromechanical fields in multi-coated long fiber composites

George Chatzigeorgiou[a], Ali Javili[b], Fodil Meraghni[a,*]

[a]*Arts et Métiers ParisTech, LEM3-UMR 7239 CNRS, 4 Rue Augustin Fresnel 57078 Metz, France*
[b]*Department of Mechanical Engineering, Bilkent University, 06800 Ankara, Turkey*

Abstract

This paper proposes a micromechanical framework for identifying the macroscopic behavior of multi-coated long fiber composites, as well as the average electromechanical microscopic fields of all phases (matrix, fibers, coating layers), generated upon known macroscopic conditions. The work aims at developing a unified micromechanical approach that provides an analytical solution standing for non-coated and multi-coated long fiber composites with transversely isotropic piezoelectric behavior. The proposed method solves specific boundary value problems and utilizes the Mori-Tanaka homogenization scheme, in which the dilute strain and electric field concentration tensors are obtained analytically with the help of an extended composite cylinders method that accounts for coupled electromechanical fields. The capabilities of this homogenization strategy are illustrated with the help of numerical examples, and comparisons with known solutions from the literature for non-coated and coated fiber piezoelectric composites are provided.

Keywords: piezoelectricity; fiber composites; multi-coated fibers; composite cylinders method.

1. Introduction

Piezoelectric materials are very attractive in applications involving the design of sensors, actuators, transducers, etc. due to their unique capability to convert electrical into mechanical energy. Using piezoelectric ceramics, like PZT, in bulk form is not always convenient, mainly due to

*Corresponding author.
Email addresses: georges.chatzigeorgiou@ensam.eu (George Chatzigeorgiou), ajavili@bilkent.edu.tr (Ali Javili), fodil.meraghni@ensam.eu (Fodil Meraghni)

their increased weight. To avoid such issues, an efficient solution is to combine these materials with non-piezoelectric polymers in the form of composites. These advanced composite materials opened new horizons in the development of new transducers and sensors with high strength, low thermal expansion coefficients, increased thermal conductivities and decreased dielectric constants.

During the last 30 years several models have been proposed in the literature to study the piezoelectric and the combined thermo-magneto-electro-elastic response of composites. Dunn and Taya (1993) have introduced an Eshelby-type approach by identifying appropriate Eshelby and concentration tensors for the combined electromechanical response. This technique later was extended to account for other phenomena, linear (Li and Dunn, 1998) and nonlinear (Hossain et al., 2015), while Zou et al. (2011) identified Eshelby tensors for arbitrary shaped piezoelectric inclusions. Benveniste (1994), based on the initial framework of Benveniste and Dvorak (1992), studied the macroscopic response of piezoelectric composites using partially the composite cylinders method. Aboudi (2001) developed a computational method for coupled electro-magneto-thermo-elastic composites and Lee et al. (2005) have proposed numerical and Eshelby-based analytical strategies for three phase electro-magneto-elastic composites. Piezoelectric composites (Berger et al., 2005, 2006; Maruccio et al., 2015), electro-magneto-thermo-elastic composites (Bravo-Castillero et al., 2009) and piezoelastic plates (Kalamkarov and Kolpakov, 2001) have been studied by using the periodic homogenization theory. A homogenization approach for studying piezoelectric composites with periodic and random microstructure was proposed by Spinelli and Lopez-Pamies (2014). Sharma et al. (2007) identified a theoretical framework that describes the conditions under which non-piezoelectric materials can be used for the design of piezoelectric nanocomposites. Ray and Batra (2009) developed a micromechanical scheme for studying piezoelectric composites with square cross section fibers, and similar technique was developed later for magneto-electro-elastic with square cross section fibers (Pakam and Arockiarajan, 2014). Koutsawa et al. (2010), using Hill's interfacial operators, proposed a self consistent scheme for studying thermo-electro-elastic properties of composites with multi-coated ellipsoidal particles. Wang et al. (2014) developed a micromechanical method for piezoelectric composites with imperfect interfaces between the ellipsoidal particles and the matrix phase, using the concept of equivalent particle. Piezoelectric

composites with imperfect interfaces have been also studied by Gu et al. (2014, 2015).

The goal of this work is to develop a unified micromechanical approach aimed at providing an analytical solution that stands for non-coated and multi-coated long fiber composites with transversely isotropic piezoelectric behavior. Studying the coating between a fiber and a matrix in composites is of vital importance. A lot of nonlinear deformation mechanisms, like plasticity and/or martensite transformation, occur frequently at a small region close to the fibers and lead to an interaction with the local damage of the fiber/matrix interface (Payandeh et al., 2010, 2012). Developing appropriate computational tools that identify the mechanical and electric fields at the proximity of the fibers can assist in the design of more accurate damage and failure criteria for piezoelectric composites.

The developed approach is based on solving specific boundary value problems, extending the composite cylinders model of Hashin and Rosen (1964). This effort can be considered as a generalization of the Dvorak and Benveniste (1992); Benveniste (1994) methodology, providing analytical expressions of the dilute strain-electric field coupled concentration tensors, which can be utilized in classical micromechanical techniques, like Mori-Tanaka or self consistent. The advantage of such information is that it permits to identify not only the overall response of the composite, but also the various average electromechanical fields generated at the matrix, the fiber and the coating layers for known macroscopic electromechanical conditions. For non-coated fibers the obtained dilute tensors are equivalent with those of Dunn and Taya (1993). To the best of the authors knowledge, the only available framework in the literature that computes concentration tensors for piezoelectric composites with coated fibers is the one of Koutsawa et al. (2010), but it is based on certain approximations. The approach discussed herein does not require such approximations, since the solution proposed in this work for the Eshelby's inhomogeneity problem is exact.

The organization of the manuscript is as follows: After the introduction, section 2 starts with a small recall on the piezoelectricity concepts, and then it describes the Mori-Tanaka type micromechanical framework and the general procedure for obtaining the dilute concentration tensors for composites with transversely isotropic piezoelectric material constituents (matrix, fiber, coating layers). Section 3 presents the case of non-coated fiber composites and discusses the consistency of the approach with published results from the open literature. Section 4 discusses the case of

coated fibers with one coating layer. Numerical examples and comparisons with existing finite element calculations and other micromechanical approaches are demonstrated in section 5. The section also includes a study in which, for given macroscopic strain and electric field and known volume fractions of the phases, all the electromechanical fields at every phase and at the overall composite are computed (Table 2). The paper finishes with a section giving some concluding remarks and future developments. For the purpose of the paper's completeness, two appendices at the end of the article provide the piezoelectric Eshelby tensor of Dunn and Taya (1993) and explain briefly the framework of Koutsawa et al. (2010).

2. Micromechanical approach for a coated fiber/matrix piezoelectric composite

2.1. General concepts from piezoelectricity and notations

In a linear piezoelectric material, the constitutive law that describes the relation between the stress tensor $\boldsymbol{\sigma}$, the electric displacement vector $\boldsymbol{D}$, the strain tensor $\boldsymbol{\varepsilon}$ and the electric field vector $\boldsymbol{E}$ is written in the following indicial form (double indices denote summation):

$$\sigma_{ij} = C_{ijkl}\varepsilon_{kl} - e_{ijm}E_m, \qquad D_i = e_{imn}\varepsilon_{mn} + \kappa_{ij}E_j.$$

In tensorial notation, the above relations are expressed as

$$\boldsymbol{\sigma} = \boldsymbol{C}:\boldsymbol{\varepsilon} - \boldsymbol{e}\cdot\boldsymbol{E}, \qquad \boldsymbol{D} = \boldsymbol{e}^T:\boldsymbol{\varepsilon} + \boldsymbol{\kappa}\cdot\boldsymbol{E}. \tag{1}$$

In the above relations $\boldsymbol{C}$ is the fourth order elasticity tensor, $\boldsymbol{\kappa}$ is the second order permittivity moduli tensor and $\boldsymbol{e}$ is the third order piezoelectric moduli tensor. The strain tensor $\boldsymbol{\varepsilon}$ and electric field vector $\boldsymbol{E}$ are related with the displacement vector $\boldsymbol{u}$ and the electric potential ϕ respectively through the relations

$$\boldsymbol{\varepsilon} = \frac{1}{2}\left[\mathrm{grad}\boldsymbol{u} + [\mathrm{grad}\boldsymbol{u}]^T\right], \qquad \boldsymbol{E} = -\mathrm{grad}\phi. \tag{2}$$

Moreover, the equilibrium and electrostatic equations read

$$\mathrm{div}\boldsymbol{\sigma} = \boldsymbol{0}, \qquad \mathrm{div}\boldsymbol{D} = 0. \tag{3}$$

Unless stated otherwise, the Voigt notation will be adopted in the sequel to represent second, third and fourth order tensors. The convention used in strains and stresses to replace the indices ij to a single index k is the following:

$$\begin{aligned} ij = 11 &\rightarrow k = 1, \qquad ij = 22 \rightarrow k = 2, \qquad ij = 33 \rightarrow k = 3, \\ ij = 12 &\rightarrow k = 4, \qquad ij = 13 \rightarrow k = 5, \qquad ij = 23 \rightarrow k = 6. \end{aligned}$$

2.2. Application of the Mori-Tanaka method

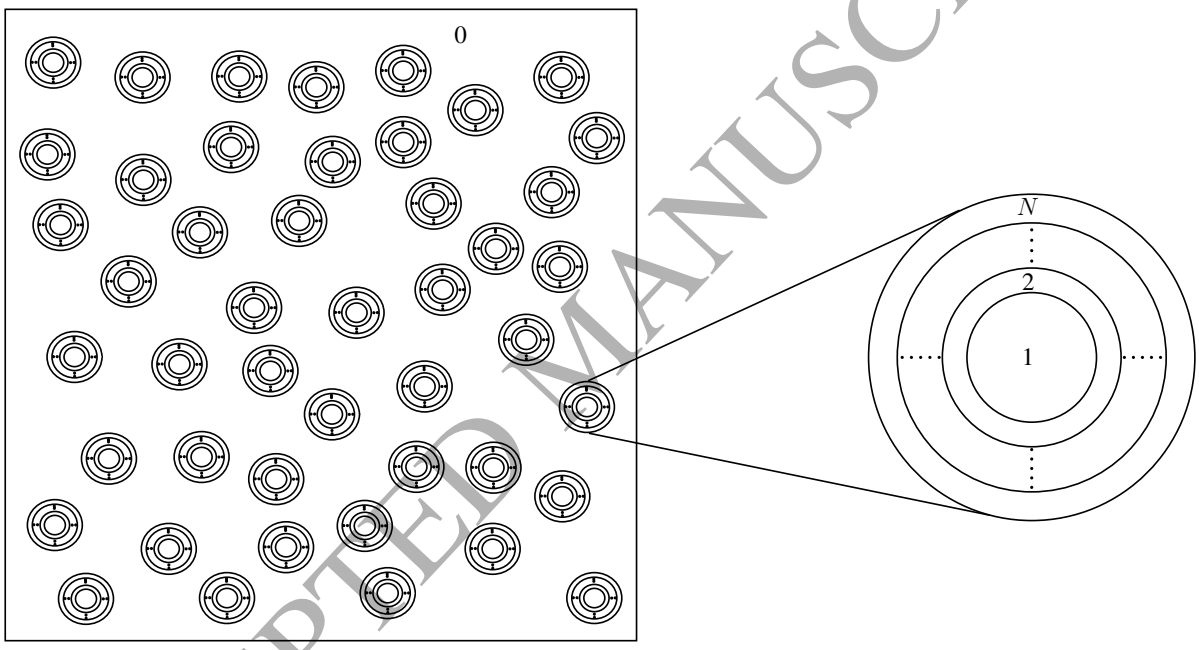

Figure 1: Unidirectional multi-coated fiber composite. The coating has $N-1$ distinct layers.

Let's consider a $N+1$-phase composite, consisting of a matrix, denoted as 0, and infinitely long, multi-coated, cylindrical fibers. The fibers are denoted with the index 1, while the $N-1$ coating layers are denoted with the indices 2,3,...,N (Figure 1). All phases are assumed to be made by linear piezoelectric materials. The phases are characterized by their piezoelectric moduli $\boldsymbol{C}_q$, $\boldsymbol{e}_q$ and $\boldsymbol{\kappa}_q$, $q = 0, 1, 2, 3, ..., N$.

According to the usual micromechanics arguments, a Representative Volume Element (RVE) with total volume V is sufficient to describe the overall response of the composite. Each phase

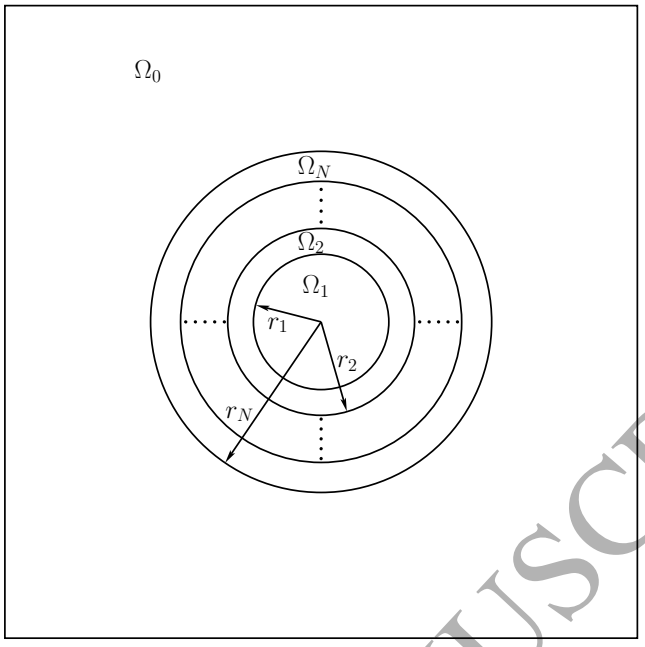

Figure 2: Typical RVE of a unidirectional multi-coated fiber composite.

in the RVE occupies the space Ω_q (Figure 2), has its own volume V_q and volume fraction c_q for $q = 0, 1, 2, 3, ..., N$. The classical volume summation rule states that

$$\sum_{q=0}^{N} V_q = V, \qquad \sum_{q=0}^{N} c_q = \sum_{q=0}^{N} \frac{V_q}{V} = 1.$$

The macroscopic strain $\overline{\boldsymbol{\varepsilon}}$, stress $\overline{\boldsymbol{\sigma}}$, electric field $\overline{\boldsymbol{E}}$ and electric displacement $\overline{\boldsymbol{D}}$ corresponding to the RVE are computed from the volume averages of their microscopic counterparts at all phases, i.e.

$$\overline{\boldsymbol{\varepsilon}} = \sum_{q=0}^{N} c_q \boldsymbol{\varepsilon}_q, \quad \overline{\boldsymbol{\sigma}} = \sum_{q=0}^{N} c_q \boldsymbol{\sigma}_q, \quad \overline{\boldsymbol{E}} = \sum_{q=0}^{N} c_q \boldsymbol{E}_q, \quad \overline{\boldsymbol{D}} = \sum_{q=0}^{N} c_q \boldsymbol{D}_q. \tag{4}$$

In these expressions $\boldsymbol{\varepsilon}_q$, $\boldsymbol{\sigma}_q$, $\boldsymbol{E}_q$ and $\boldsymbol{D}_q$ denote the average strain, stress, electric field and electric displacement in the q_{th} phase respectively:

$$\boldsymbol{\varepsilon}_q = \frac{1}{V_q}\int_{\Omega_q} \boldsymbol{\varepsilon}(\boldsymbol{x})\,\mathrm{d}V, \quad \boldsymbol{\sigma}_q = \frac{1}{V_q}\int_{\Omega_q} \boldsymbol{\sigma}(\boldsymbol{x})\,\mathrm{d}V, \quad \boldsymbol{E}_q = \frac{1}{V_q}\int_{\Omega_q} \boldsymbol{E}(\boldsymbol{x})\,\mathrm{d}V, \quad \boldsymbol{D}_q = \frac{1}{V_q}\int_{\Omega_q} \boldsymbol{D}(\boldsymbol{x})\,\mathrm{d}V. \tag{5}$$

The constitutive law of each phase states that

$$\boldsymbol{\sigma}_q = \boldsymbol{C}_q{:}\boldsymbol{\varepsilon}_q - \boldsymbol{e}_q{\cdot}\boldsymbol{E}_q, \quad \boldsymbol{D}_q = \boldsymbol{e}_q^T{:}\boldsymbol{\varepsilon}_q + \boldsymbol{\kappa}_q{\cdot}\boldsymbol{E}_q, \quad q = 0, 1, 2, 3, ..., N. \tag{6}$$

The goal of homogenization is to identify a similar type of constitutive law for the macroscopic quantities, i.e.

$$\bar{\boldsymbol{\sigma}} = \bar{\boldsymbol{C}}:\bar{\boldsymbol{\varepsilon}} - \bar{\boldsymbol{e}}\cdot\bar{\boldsymbol{E}}, \quad \bar{\boldsymbol{D}} = \bar{\boldsymbol{e}}^T:\bar{\boldsymbol{\varepsilon}} + \bar{\boldsymbol{\kappa}}\cdot\bar{\boldsymbol{E}}, \tag{7}$$

where $\bar{\boldsymbol{C}}$, $\bar{\boldsymbol{\kappa}}$ and $\bar{\boldsymbol{e}}$ are the macroscopic elasticity, permittivity and piezoelectric tensors respectively.[1] The law (7) represents the overall behavior of the composite. According to the Mori-Tanaka approach, the average fields in the fiber or the coatings and the matrix phase ($q = 0$) are connected to each other through the dilute concentration tensors:

$$\boldsymbol{\varepsilon}_q = \boldsymbol{T}_q^{mm}:\boldsymbol{\varepsilon}_0 + \boldsymbol{T}_q^{me}\cdot\boldsymbol{E}_0, \quad \boldsymbol{E}_q = \boldsymbol{T}_q^{em}:\boldsymbol{\varepsilon}_0 + \boldsymbol{T}_q^{ee}\cdot\boldsymbol{E}_0, \quad q = 1, 2, 3, ..., N. \tag{8}$$

$\boldsymbol{T}_q^{mm}$ are fourth order tensors, written as 6×6 matrices, $\boldsymbol{T}_q^{me}$ are third order tensors, written as 6×3 matrices, $\boldsymbol{T}_q^{em}$ are third order tensors, written as 3×6 matrices and $\boldsymbol{T}_q^{ee}$ are second order tensors, written as 3×3 matrices. Combining (8) with $(4)_{1,3}$ and after some algebra, the following relations are obtained:

$$\boldsymbol{\varepsilon}_q = \boldsymbol{A}_q^{mm}:\bar{\boldsymbol{\varepsilon}} + \boldsymbol{A}_q^{me}\cdot\bar{\boldsymbol{E}}, \quad \boldsymbol{E}_q = \boldsymbol{A}_q^{em}:\bar{\boldsymbol{\varepsilon}} + \boldsymbol{A}_q^{ee}\cdot\bar{\boldsymbol{E}}, \quad q = 0, 1, 2, 3, ..., N, \tag{9}$$

where

$$\begin{aligned} \boldsymbol{A}_0^{mm} &= \left[\boldsymbol{\Pi}^{mm} - \boldsymbol{\Pi}^{me}\cdot[\boldsymbol{\Pi}^{ee}]^{-1}\cdot\boldsymbol{\Pi}^{em}\right]^{-1}, \quad \boldsymbol{A}_0^{me} = -\boldsymbol{A}_0^{mm}:\boldsymbol{\Pi}^{me}\cdot[\boldsymbol{\Pi}^{ee}]^{-1}, \\ \boldsymbol{A}_0^{em} &= -[\boldsymbol{\Pi}^{ee}]^{-1}\cdot\boldsymbol{\Pi}^{em}:\boldsymbol{A}_0^{mm}, \quad \boldsymbol{A}_0^{ee} = [\boldsymbol{\Pi}^{ee}]^{-1} - [\boldsymbol{\Pi}^{ee}]^{-1}:\boldsymbol{\Pi}^{em}:\boldsymbol{A}_0^{me}, \end{aligned} \tag{10}$$

and

$$\begin{aligned} \boldsymbol{A}_q^{mm} &= \boldsymbol{T}_q^{mm}:\boldsymbol{A}_0^{mm} + \boldsymbol{T}_q^{me}\cdot\boldsymbol{A}_0^{em}, \quad \boldsymbol{A}_q^{me} = \boldsymbol{T}_q^{mm}:\boldsymbol{A}_0^{me} + \boldsymbol{T}_q^{me}\cdot\boldsymbol{A}_0^{ee}, \\ \boldsymbol{A}_q^{em} &= \boldsymbol{T}_q^{em}:\boldsymbol{A}_0^{mm} + \boldsymbol{T}_q^{ee}\cdot\boldsymbol{A}_0^{em}, \quad \boldsymbol{A}_q^{ee} = \boldsymbol{T}_q^{em}:\boldsymbol{A}_0^{me} + \boldsymbol{T}_q^{ee}\cdot\boldsymbol{A}_0^{ee}, \end{aligned} \tag{11}$$

for $q = 1, 2, 3, ..., N$. In the above relations,

$$\boldsymbol{\Pi}^{mm} = c_0\boldsymbol{\mathcal{I}} + \sum_{q=1}^{N} c_q\boldsymbol{T}_q^{mm}, \quad \boldsymbol{\Pi}^{me} = \sum_{q=1}^{N} c_q\boldsymbol{T}_q^{me}, \quad \boldsymbol{\Pi}^{em} = \sum_{q=1}^{N} c_q\boldsymbol{T}_q^{em}, \quad \boldsymbol{\Pi}^{ee} = c_0\boldsymbol{I} + \sum_{q=1}^{N} c_q\boldsymbol{T}_q^{ee}, \tag{12}$$

[1] Contrarily to the electromechanical fields, the macroscopic moduli are generally not equal to the volume averages of their microscopic counterparts. The Voigt bound, which considers such relation, often provides a poor estimate of the real response.

while $\boldsymbol{\mathcal{I}}$ and $\boldsymbol{I}$, with

$$[\boldsymbol{\mathcal{I}}]_{ijkl} = \frac{1}{2}[\delta_{ik}\delta_{jl} + \delta_{il}\delta_{jk}], \quad [\boldsymbol{I}]_{ij} = \delta_{ij}, \quad \delta_{ij}\text{: Kronecker delta,}$$

denote the symmetric fourth order and second order identity tensors respectively. Substituting (9) in (6) gives

$$\begin{aligned} \boldsymbol{\sigma}_q &= \left[\boldsymbol{C}_q : \boldsymbol{A}_q^{mm} - \boldsymbol{\varepsilon}_q \cdot \boldsymbol{A}_q^{em}\right]\bar{\boldsymbol{\varepsilon}} - \left[\boldsymbol{e}_q \cdot \boldsymbol{A}_q^{ee} - \boldsymbol{C}_q : \boldsymbol{A}_q^{me}\right]\bar{\boldsymbol{E}}, \\ \boldsymbol{D}_q &= \left[\boldsymbol{e}_q^T : \boldsymbol{A}_q^{mm} + \boldsymbol{\kappa}_q \cdot \boldsymbol{A}_q^{em}\right]\bar{\boldsymbol{\varepsilon}} + \left[\boldsymbol{e}_q^T : \boldsymbol{A}_q^{me} + \boldsymbol{\kappa}_q \cdot \boldsymbol{A}_q^{ee}\right]\bar{\boldsymbol{E}}, \end{aligned} \tag{13}$$

for $q = 0, 1, 2, 3, ..., N$. Implementing these results in $(4)_{2,4}$ and comparing with (7) eventually yields

$$\begin{aligned} \bar{\boldsymbol{C}} &= \sum_{q=0}^{N} c_q \left[\boldsymbol{C}_q : \boldsymbol{A}_q^{mm} - \boldsymbol{\varepsilon}_q \cdot \boldsymbol{A}_q^{em}\right], \qquad \bar{\boldsymbol{e}} = \sum_{q=0}^{N} c_q \left[\boldsymbol{e}_q \cdot \boldsymbol{A}_q^{ee} - \boldsymbol{C}_q : \boldsymbol{A}_q^{me}\right], \\ \bar{\boldsymbol{e}}^T &= \sum_{q=0}^{N} c_q \left[\boldsymbol{e}_q^T : \boldsymbol{A}_q^{mm} + \boldsymbol{\kappa}_q \cdot \boldsymbol{A}_q^{em}\right], \qquad \bar{\boldsymbol{\kappa}} = \sum_{q=0}^{N} c_q \left[\boldsymbol{e}_q^T : \boldsymbol{A}_q^{me} + \boldsymbol{\kappa}_q \cdot \boldsymbol{A}_q^{ee}\right]. \end{aligned} \tag{14}$$

Of course, the forms of the dilute concentration tensors $\boldsymbol{T}_q^{mm}$, $\boldsymbol{T}_q^{me}$, $\boldsymbol{T}_q^{em}$ and $\boldsymbol{T}_q^{ee}$ should respect the compatibility between the equations $(14)_2$ and $(14)_3$.

It is worth mentioning that it is possible to construct one single dilute concentration tensor that combines the four tensors of the expressions (8) (see for instance Dunn and Taya, 1993). The advantage of using separate dilute tensors for each field (mechanical and electrical) and the couplings arising from them is that the scheme can be extended more naturally to account for additional mechanisms. Indeed, one can obtain dilute concentration tensors for thermomechanical response (Benveniste et al., 1991; Chatzigeorgiou et al., 2018), or for inelastic response, like in the case of the Transformation Field Analysis approach (Dvorak and Benveniste, 1992; Dvorak, 1992).

2.3. Dilute piezoelectric concentration tensors

For the identification of the dilute concentration tensors, a single linear piezoelectric coated fiber is assumed to be embedded inside the linear piezoelectric matrix, as shown in Figure 3.

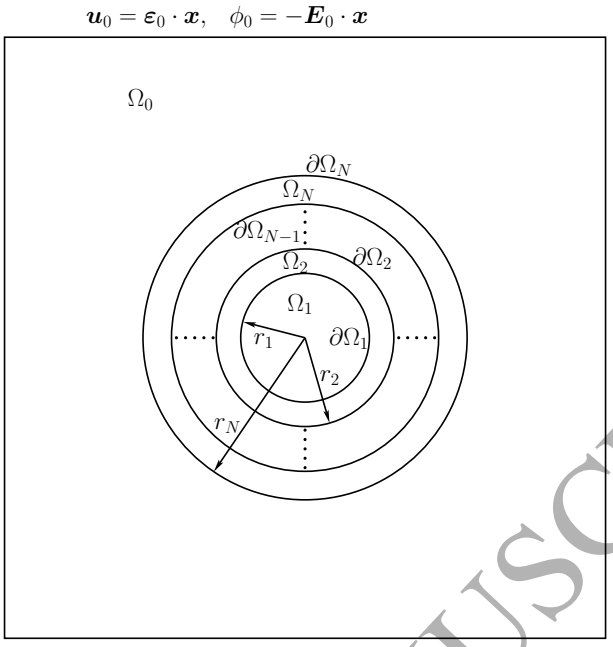

Figure 3: Coated fiber inside a matrix, subjected to linear displacement and electric potential at far distance. All phases are piezoelectric materials.

The fiber occupies the space Ω_1 with volume V_1, its coatings the spaces Ω_q with volumes V_q, $q = 2, 3, ..., N$ and the matrix occupies the space Ω_0, which is extended to far distance from the fiber. The matrix is subjected to linear displacement $\boldsymbol{u}_0 = \boldsymbol{\varepsilon}_0 \cdot \boldsymbol{x}$ and linear electric potential $\phi_0 = -\boldsymbol{E}_0 \cdot \boldsymbol{x}$ at far distance from the fiber ($r \to \infty$). The interface between each phase is considered perfect. The interface between the phase q and the phase $q + 1$ for $q = 1, ..., N - 1$ is denoted as $\partial\Omega_q$, while the interface between the last coating layer and the matrix is denotes as $\partial\Omega_N$.

The various electromechanical fields generated at every phase q depend on the spatial position, i.e.

$$\boldsymbol{u}^{(q)}(\boldsymbol{x}), \quad \boldsymbol{\varepsilon}^{(q)}(\boldsymbol{x}), \quad \boldsymbol{\sigma}^{(q)}(\boldsymbol{x}), \quad \phi^{(q)}(\boldsymbol{x}), \quad \boldsymbol{E}^{(q)}(\boldsymbol{x}), \quad \boldsymbol{D}^{(q)}(\boldsymbol{x}), \qquad \forall \boldsymbol{x} \in \Omega_q. \tag{15}$$

In infinitely long fiber composites, it is more convenient to describe all the necessary equations in cylindrical coordinates, by describing the position vector in terms of the radius r, the angle θ and the longitudinal position z (Figure 4). For transversely isotropic piezoelectric matrix, fiber and

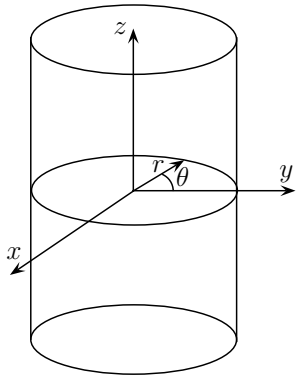

Figure 4: Cylindrical coordinate system.

coatings, the constitutive law (6) for each phase is written in Voigt notation as

$$\begin{bmatrix} \sigma_{rr}^{(q)} \\ \sigma_{\theta\theta}^{(q)} \\ \sigma_{zz}^{(q)} \\ \sigma_{r\theta}^{(q)} \\ \sigma_{rz}^{(q)} \\ \sigma_{\theta z}^{(q)} \end{bmatrix} = \begin{bmatrix} K_q^{\mathrm{tr}}+\mu_q^{\mathrm{tr}} & K_q^{\mathrm{tr}}-\mu_q^{\mathrm{tr}} & l_q & 0 & 0 & 0 \\ K_q^{\mathrm{tr}}-\mu_q^{\mathrm{tr}} & K_q^{\mathrm{tr}}+\mu_q^{\mathrm{tr}} & l_q & 0 & 0 & 0 \\ l_q & l_q & n_q & 0 & 0 & 0 \\ 0 & 0 & 0 & \mu_q^{\mathrm{tr}} & 0 & 0 \\ 0 & 0 & 0 & 0 & \mu_q^{\mathrm{ax}} & 0 \\ 0 & 0 & 0 & 0 & 0 & \mu_q^{\mathrm{ax}} \end{bmatrix} \cdot \begin{bmatrix} \varepsilon_{rr}^{(q)} \\ \varepsilon_{\theta\theta}^{(q)} \\ \varepsilon_{zz}^{(q)} \\ 2\varepsilon_{r\theta}^{(q)} \\ 2\varepsilon_{rz}^{(q)} \\ 2\varepsilon_{\theta z}^{(q)} \end{bmatrix} - \begin{bmatrix} 0 & 0 & e_{q_{31}} \\ 0 & 0 & e_{q_{31}} \\ 0 & 0 & e_{q_{33}} \\ 0 & 0 & 0 \\ e_{q_{15}} & 0 & 0 \\ 0 & e_{q_{15}} & 0 \end{bmatrix} \cdot \begin{bmatrix} E_r^{(q)} \\ E_\theta^{(q)} \\ E_z^{(q)} \end{bmatrix}, \quad (16)$$

$$\begin{bmatrix} D_r^{(q)} \\ D_\theta^{(q)} \\ D_z^{(q)} \end{bmatrix} = \begin{bmatrix} 0 & 0 & 0 & 0 & e_{q15} & 0 \\ 0 & 0 & 0 & 0 & 0 & e_{q15} \\ e_{q31} & e_{q31} & e_{q33} & 0 & 0 & 0 \end{bmatrix} \cdot \begin{bmatrix} \varepsilon_{rr}^{(q)} \\ \varepsilon_{\theta\theta}^{(q)} \\ \varepsilon_{zz}^{(q)} \\ 2\varepsilon_{r\theta}^{(q)} \\ 2\varepsilon_{rz}^{(q)} \\ 2\varepsilon_{\theta z}^{(q)} \end{bmatrix} + \begin{bmatrix} \kappa_{q11} & 0 & 0 \\ 0 & \kappa_{q11} & 0 \\ 0 & 0 & \kappa_{q33} \end{bmatrix} \cdot \begin{bmatrix} E_r^{(q)} \\ E_\theta^{(q)} \\ E_z^{(q)} \end{bmatrix}. \quad (17)$$

The strain tensor and the electric field vector at each phase are given by the expressions

$$\begin{aligned} \varepsilon_{rr}^{(q)} &= \frac{\partial u_r^{(q)}}{\partial r}, \quad \varepsilon_{\theta\theta}^{(q)} = \frac{1}{r}\frac{\partial u_\theta^{(q)}}{\partial \theta} + \frac{u_r^{(q)}}{r}, \quad \varepsilon_{zz}^{(q)} = \frac{\partial u_z^{(q)}}{\partial z}, \\ 2\varepsilon_{rz}^{(q)} &= \frac{\partial u_z^{(q)}}{\partial r} + \frac{\partial u_r^{(q)}}{\partial z}, \quad 2\varepsilon_{\theta z}^{(q)} = \frac{1}{r}\frac{\partial u_z^{(q)}}{\partial \theta} + \frac{\partial u_\theta^{(q)}}{\partial z}, \quad 2\varepsilon_{r\theta}^{(q)} = \frac{\partial u_\theta^{(q)}}{\partial r} + \frac{1}{r}\frac{\partial u_r^{(q)}}{\partial \theta} - \frac{u_\theta^{(q)}}{r}, \\ E_r^{(q)} &= -\frac{\partial \phi^{(q)}}{\partial r}, \quad E_\theta^{(q)} = -\frac{1}{r}\frac{\partial \phi^{(q)}}{\partial \theta}, \quad E_z^{(q)} = -\frac{\partial \phi^{(q)}}{\partial z}, \end{aligned} \quad (18)$$

while the equilibrium and electrostatic equations are written as

$$\begin{aligned} \frac{\partial \sigma_{rr}^{(q)}}{\partial r} + \frac{1}{r}\frac{\partial \sigma_{r\theta}^{(q)}}{\partial \theta} + \frac{\sigma_{rr}^{(q)} - \sigma_{\theta\theta}^{(q)}}{r} + \frac{\partial \sigma_{rz}^{(q)}}{\partial z} &= 0, \\ \frac{\partial \sigma_{r\theta}^{(q)}}{\partial r} + \frac{1}{r}\frac{\partial \sigma_{\theta\theta}^{(q)}}{\partial \theta} + \frac{2\sigma_{r\theta}^{(q)}}{r} + \frac{\partial \sigma_{\theta z}^{(q)}}{\partial z} &= 0, \\ \frac{\partial \sigma_{rz}^{(q)}}{\partial r} + \frac{1}{r}\frac{\partial \sigma_{\theta z}^{(q)}}{\partial \theta} + \frac{\sigma_{rz}^{(q)}}{r} + \frac{\partial \sigma_{zz}^{(q)}}{\partial z} &= 0, \\ \frac{\partial D_r^{(q)}}{\partial r} + \frac{1}{r}\frac{\partial D_\theta^{(q)}}{\partial \theta} + \frac{D_r^{(q)}}{r} + \frac{\partial D_z^{(q)}}{\partial z} &= 0. \end{aligned} \quad (19)$$

The fiber is considered to have radius $r = r_1$ and every coating q has external radius r_q (Figure 3). The interface conditions between the phase q and the phase $q+1$ for $q = 1, 2, 3, ..., N-1$ are

expressed as

$$u_r^{(q)}(r_q,\theta,z) = u_r^{(q+1)}(r_q,\theta,z), \quad u_\theta^{(q)}(r_q,\theta,z) = u_\theta^{(q+1)}(r_q,\theta,z), \quad u_z^{(q)}(r_q,\theta,z) = u_z^{(q+1)}(r_q,\theta,z),$$
$$\sigma_{rr}^{(q)}(r_q,\theta,z) = \sigma_{rr}^{(q+1)}(r_q,\theta,z), \quad \sigma_{r\theta}^{(q)}(r_q,\theta,z) = \sigma_{r\theta}^{(q+1)}(r_q,\theta,z), \quad \sigma_{rz}^{(q)}(r_q,\theta,z) = \sigma_{rz}^{(q+1)}(r_q,\theta,z),$$
$$\phi^{(q)}(r_q,\theta,z) = \phi^{(q+1)}(r_q,\theta,z), \quad D_r^{(q)}(r_q,\theta,z) = D_r^{(q+1)}(r_q,\theta,z). \quad (20)$$

Additionally, the interface conditions between the N_{th} coating and the matrix are written as

$$u_r^{(N)}(r_N,\theta,z) = u_r^{(0)}(r_N,\theta,z), \quad u_\theta^{(N)}(r_N,\theta,z) = u_\theta^{(0)}(r_N,\theta,z), \quad u_z^{(N)}(r_N,\theta,z) = u_z^{(0)}(r_N,\theta,z),$$
$$\sigma_{rr}^{(N)}(r_N,\theta,z) = \sigma_{rr}^{(0)}(r_N,\theta,z), \quad \sigma_{r\theta}^{(N)}(r_N,\theta,z) = \sigma_{r\theta}^{(0)}(r_N,\theta,z), \quad \sigma_{rz}^{(N)}(r_N,\theta,z) = \sigma_{rz}^{(0)}(r_N,\theta,z),$$
$$\phi^{(N)}(r_N,\theta,z) = \phi^{(0)}(r_N,\theta,z), \quad D_r^{(N)}(r_N,\theta,z) = D_r^{(0)}(r_N,\theta,z). \quad (21)$$

Following the Eshelby's methodology, the dilute concentration tensors provide the relationship between the average strain $\boldsymbol{\varepsilon}_q$ and electric field $\boldsymbol{E}_q$ inside the phase q ($q = 1, 2, 3, ..., N$), and the strain $\boldsymbol{\varepsilon}_0$ and electric field $\boldsymbol{E}_0$ at the far field:

$$\boldsymbol{\varepsilon}_q = \boldsymbol{T}_q^{mm} : \boldsymbol{\varepsilon}_0 + \boldsymbol{T}_q^{me} \cdot \boldsymbol{E}_0, \quad \boldsymbol{E}_q = \boldsymbol{T}_q^{em} : \boldsymbol{\varepsilon}_0 + \boldsymbol{T}_q^{ee} \cdot \boldsymbol{E}_0. \quad (22)$$

The Mori-Tanaka approach assumes that the strain $\boldsymbol{\varepsilon}_0$ and the electric field $\boldsymbol{E}_0$ applied in the far field of this Eshelby-type problem correspond to the average strain $\boldsymbol{\varepsilon}_0$ and the average electric field $\boldsymbol{E}_0$ of the matrix in the RVE of Figure 2, which are used in equations (8). Using the divergence theorem, one obtains for the fiber the average fields

$$\begin{aligned} \boldsymbol{\varepsilon}_1 &= \frac{1}{V_1}\int_{\Omega_1} \boldsymbol{\varepsilon}^{(1)}\,\mathrm{d}V = \frac{1}{V_1}\int_{\partial\Omega_1} \frac{1}{2}[\boldsymbol{u}^{(1)} \otimes \boldsymbol{n} + \boldsymbol{n} \otimes \boldsymbol{u}^{(1)}]\,\mathrm{d}S, \\ \boldsymbol{E}_1 &= \frac{1}{V_1}\int_{\Omega_1} \boldsymbol{E}^{(1)}\,\mathrm{d}V = \frac{1}{V_1}\int_{\partial\Omega_1} [-\phi^{(1)}]\boldsymbol{n}\,\mathrm{d}S, \end{aligned} \quad (23)$$

where $\boldsymbol{n}$ is the unit vector of the interface $\partial\Omega_1$. Due to the homothetic topology of the coated fiber, the unit vector is the same at all interfaces. For all the coating layers, the average strain and electric field are defined as

$$\begin{aligned} \boldsymbol{\varepsilon}_q = \frac{1}{V_q}\int_{\Omega_q} \boldsymbol{\varepsilon}^{(q)}\,\mathrm{d}V &= \frac{1}{V_q}\int_{\partial\Omega_q} \frac{1}{2}[\boldsymbol{u}^{(q)} \otimes \boldsymbol{n} + \boldsymbol{n} \otimes \boldsymbol{u}^{(q)}]\,\mathrm{d}S \\ &\quad - \frac{1}{V_q}\int_{\partial\Omega_{q-1}} \frac{1}{2}[\boldsymbol{u}^{(q-1)} \otimes \boldsymbol{n} + \boldsymbol{n} \otimes \boldsymbol{u}^{(q-1)}]\,\mathrm{d}S, \\ \boldsymbol{E}_q = \frac{1}{V_q}\int_{\Omega_q} \boldsymbol{E}^{(q)}\,\mathrm{d}V &= \frac{1}{V_q}\left[\int_{\partial\Omega_q} [-\phi^{(q)}]\boldsymbol{n}\,\mathrm{d}S - \int_{\partial\Omega_{q-1}} [-\phi^{(q-1)}]\boldsymbol{n}\,\mathrm{d}S\right]. \end{aligned} \quad (24)$$

Obtaining the dilute piezoelectric tensors is not an easy task. For certain, ellipsoidal-type, forms of inclusions without coating, Dunn and Taya (1993) have computed the Eshelby tensors for the combined strain/electric field system (see Appendix A for infinitely long fibers). In the present work, the dilute concentration tensors are computed directly for long coated fiber piezoelectric composites with transversely isotropic behavior at every phase. To achieve such goal, analytical solutions are utilized of similar boundary value problems with those of the composite cylinders method proposed by Hashin (1990), taking into account the effects caused by the combined presence of mechanical and electric fields. In the pure mechanical problem, similar techniques have been utilized in the literature to obtain dilute (Benveniste et al., 1989) and semi-dilute (Chatzigeorgiou et al., 2012) stress concentration tensors, as well as dilute strain concentration tensors (Wang et al., 2016) for coated fiber composites.

In cylindrical coordinates, the surface element in a surface of constant radius r (a vertical cylinder) is $\mathrm{d}s_r = r\mathrm{d}\theta\mathrm{d}z$ and the surface element in a surface of constant z is $\mathrm{d}s_z = r\mathrm{d}r\mathrm{d}\theta$. For an arbitrary tensor $\boldsymbol{Q}(r,\theta,z)$ and a cylinder of radius r_q and length $2L$, the sum of surface integrals with the general form

$$\mathcal{F} = \frac{1}{2L\pi r_q}\int_{-L}^{L}\int_{0}^{2\pi}\boldsymbol{Q}(r_q,\theta,z)\mathrm{d}\theta\mathrm{d}z + \frac{1}{2L\pi r_q^2}\int_{0}^{2\pi}\int_{0}^{r_q}\left[\boldsymbol{Q}(r,\theta,L)-\boldsymbol{Q}(r,\theta,-L)\right] r\mathrm{d}r\mathrm{d}\theta\,, \quad (25)$$

is required for the computations of the average quantities (23) and (24)[2]. The three normal vectors in cylindrical coordinates are expressed as

$$\boldsymbol{n}_1 = \begin{bmatrix}\cos\theta\\ \sin\theta\\ 0\end{bmatrix},\quad \boldsymbol{n}_2 = \begin{bmatrix}-\sin\theta\\ \cos\theta\\ 0\end{bmatrix},\quad \boldsymbol{n}_3 = \begin{bmatrix}0\\ 0\\ 1\end{bmatrix}. \quad (26)$$

The displacements of the phases are represented in matrix form as

$$\boldsymbol{u}^{(q)} = u_r^{(q)}\,\boldsymbol{n}_1 + u_\theta^{(q)}\,\boldsymbol{n}_2 + u_z^{(q)}\,\boldsymbol{n}_3. \quad (27)$$

Another important point to be mentioned is that in long fiber composites with, at most, transversely isotropic phases (axis of symmetry: the direction of fibers), the dilute strain concentration tensors

[2]For infinitely long cylinder, $L\to\infty$. To avoid infinite values, the division by volume takes care of L.

present transverse isotropy. In Voigt notation, they take the form

$$\boldsymbol{T}_q^{mm} = \begin{bmatrix} T_{q11}^{mm} & T_{q11}^{mm}-T_{q44}^{mm} & T_{q13}^{mm} & 0 & 0 & 0 \\ T_{q11}^{mm}-T_{q44}^{mm} & T_{q11}^{mm} & T_{q13}^{mm} & 0 & 0 & 0 \\ 0 & 0 & 1 & 0 & 0 & 0 \\ 0 & 0 & 0 & T_{q44}^{mm} & 0 & 0 \\ 0 & 0 & 0 & 0 & T_{q55}^{mm} & 0 \\ 0 & 0 & 0 & 0 & 0 & T_{q55}^{mm} \end{bmatrix}, \quad \boldsymbol{T}_q^{me} = \begin{bmatrix} 0 & 0 & T_{q31}^{me} \\ 0 & 0 & T_{q31}^{me} \\ 0 & 0 & 0 \\ 0 & 0 & 0 \\ T_{q15}^{me} & 0 & 0 \\ 0 & T_{q15}^{me} & 0 \end{bmatrix},$$

$$\boldsymbol{T}_q^{em} = \begin{bmatrix} 0 & 0 & 0 & 0 & T_{q15}^{em} & 0 \\ 0 & 0 & 0 & 0 & 0 & T_{q15}^{em} \\ 0 & 0 & 0 & 0 & 0 & 0 \end{bmatrix}, \quad \boldsymbol{T}_q^{ee} = \begin{bmatrix} T_{q11}^{ee} & 0 & 0 \\ 0 & T_{q11}^{ee} & 0 \\ 0 & 0 & 1 \end{bmatrix}. \tag{28}$$

To obtain the unknown terms of these tensors, four types of boundary value problems should be examined. In the sequel two cases are studied: a fiber/matrix composite without coating and a fiber/matrix composite with only one coating layer.

3. First case: non-coated fibers

The first studied case considers non-coated piezoelectric fibers embedded in a piezoelectric matrix. This is a well examined problem in the literature and the scope of this section is to illustrate that the proposed methodology produces reliable results.

3.1. Axial shear strain and in-plane electric field conditions

For this case the following displacement vector and electric potential are applied:

$$\boldsymbol{u}_0^{(x,y,z)} = \begin{bmatrix} 0 \\ 0 \\ \beta x \end{bmatrix}, \qquad \phi_0^{(x,y,z)} = -\gamma x. \tag{29}$$

These correspond to the following strain tensor (in classical tensorial form) and electric field vector

$$\boldsymbol{\varepsilon}_0 = \begin{bmatrix} 0 & 0 & \beta/2 \\ 0 & 0 & 0 \\ \beta/2 & 0 & 0 \end{bmatrix}, \qquad \boldsymbol{E}_0 = \begin{bmatrix} \gamma \\ 0 \\ 0 \end{bmatrix}.$$

In cylindrical coordinates, the displacement and electric potential are transformed to

$$\boldsymbol{u}_0^{(r,\theta,z)} = \begin{bmatrix} 0 \\ 0 \\ \beta r \cos\theta \end{bmatrix}, \qquad \phi_0^{(r,\theta,z)} = -\gamma r \cos\theta.$$

For these boundary conditions, the displacement vector and electric potential at the matrix ($q = 0$) and the fiber ($q = 1$) are given by the general expressions

$$\begin{aligned} u_z^{(q)}(r,\theta) &= \beta r U_z^{(q)}(r)\cos\theta, \qquad u_r^{(q)} = u_\theta^{(q)} = 0, \qquad U_z^{(q)}(r) = \Xi_1^{(q)} + \Xi_2^{(q)} \frac{1}{[r/r_1]^2}, \\ \phi^{(q)}(r,\theta) &= -\gamma r \Phi^{(q)}(r)\cos\theta, \qquad \Phi^{(q)}(r) = \Xi_3^{(q)} + \Xi_4^{(q)} \frac{1}{[r/r_1]^2}. \end{aligned} \tag{30}$$

where $\Xi_i^{(q)}$, $i = 1, 2, 3, 4$, are unknown constants. These general expressions lead to stresses and electric displacements that satisfy the equilibrium and electrostatic equations (19). The important stresses and electric displacements for identifying the unknown constants are

$$\sigma_{rz}^{(q)}(r,\theta) = \left[\beta\, \Sigma_{rz}^{m(q)}(r) + \gamma\, \Sigma_{rz}^{e(q)}(r)\right]\cos\theta, \qquad D_r^{(q)}(r,\theta) = \left[\beta\, D_r^{m(q)}(r) + \gamma\, D_r^{e(q)}(r)\right]\cos\theta,$$

$$\Sigma_{rz}^{m(q)}(r) = \mu_q^{\mathrm{ax}} \left[\Xi_1^{(q)} - \Xi_2^{(q)} \frac{1}{[r/r_1]^2}\right], \qquad \Sigma_{rz}^{e(q)}(r) = -e_{q_{15}} \left[\Xi_3^{(q)} - \Xi_4^{(q)} \frac{1}{[r/r_1]^2}\right],$$

$$D_r^{m(q)}(r) = e_{q_{15}} \left[\Xi_1^{(q)} - \Xi_2^{(q)} \frac{1}{[r/r_1]^2}\right], \qquad D_r^{e(q)}(r) = \kappa_{q_{11}} \left[\Xi_3^{(q)} - \Xi_4^{(q)} \frac{1}{[r/r_1]^2}\right].$$

The boundary conditions that should be satisfied in this boundary value problem are

$$\begin{aligned} & u_z^{(1)} \text{ and } \phi^{(1)} \text{ finite at } r = 0 \quad \rightarrow \quad \Xi_2^{(1)} = \Xi_4^{(1)} = 0, \\ & u_z^{(0)}(r \rightarrow \infty, \theta) = \beta r \cos\theta \text{ and } \phi^{(0)}(r \rightarrow \infty, \theta) = -\gamma r \cos\theta \quad \rightarrow \quad \Xi_1^{(0)} = \Xi_3^{(0)} = 1\,. \end{aligned} \tag{31}$$

Considering these results, the interface conditions

$$u_z^{(1)}(r_1,\theta) = u_z^{(0)}(r_1,\theta), \quad \sigma_{rz}^{(1)}(r_1,\theta) = \sigma_{rz}^{(0)}(r_1,\theta), \quad \phi^{(1)}(r_1,\theta) = \phi^{(0)}(r_1,\theta), \quad D_r^{(1)}(r_1,\theta) = D_r^{(0)}(r_1,\theta),$$

construct the linear system

$$\boldsymbol{K}\cdot\left[\beta\,\boldsymbol{I}^{m}+\gamma\,\boldsymbol{I}^{e}\right]\cdot\left[\boldsymbol{\Xi}^{m}+\boldsymbol{\Xi}^{e}\right]=\beta\,\boldsymbol{F}_{\beta}+\gamma\,\boldsymbol{F}_{\gamma},$$

with

$$\begin{aligned}
\boldsymbol{K} &= \begin{bmatrix} 1 & -1 & 0 & 0 \\ \mu_1^{\mathrm{ax}} & \mu_0^{\mathrm{ax}} & -e_{1_{15}} & -e_{0_{15}} \\ 0 & 0 & 1 & -1 \\ e_{1_{15}} & e_{0_{15}} & \kappa_{1_{11}} & \kappa_{0_{11}} \end{bmatrix}, \quad \boldsymbol{I}^{m} = \begin{bmatrix} 1 & 0 & 0 & 0 \\ 0 & 1 & 0 & 0 \\ 0 & 0 & 0 & 0 \\ 0 & 0 & 0 & 0 \end{bmatrix}, \quad \boldsymbol{I}^{e} = \begin{bmatrix} 0 & 0 & 0 & 0 \\ 0 & 0 & 0 & 0 \\ 0 & 0 & 1 & 0 \\ 0 & 0 & 0 & 1 \end{bmatrix}, \\
\boldsymbol{\Xi}^{m} &= \begin{bmatrix} \Xi_1^{(1)} & \Xi_2^{(0)} & 0 & 0 \end{bmatrix}^{T}, \quad \boldsymbol{\Xi}^{e} = \begin{bmatrix} 0 & 0 & \Xi_3^{(1)} & \Xi_4^{(0)} \end{bmatrix}^{T}, \\
\boldsymbol{F}_{\beta} &= \begin{bmatrix} 1 & \mu_0^{\mathrm{ax}} & 0 & e_{0_{15}} \end{bmatrix}^{T}, \quad \boldsymbol{F}_{\gamma} = \begin{bmatrix} 0 & -e_{0_{15}} & 1 & \kappa_{0_{11}} \end{bmatrix}^{T}.
\end{aligned}$$

The solution of this linear system is written in the form

$$\boldsymbol{\Xi}^{m}=\boldsymbol{I}^{m}\cdot\left[\boldsymbol{K}^{-1}\cdot\boldsymbol{F}_{\beta}+\frac{\gamma}{\beta}\boldsymbol{K}^{-1}\cdot\boldsymbol{F}_{\gamma}\right],\quad \boldsymbol{\Xi}^{e}=\boldsymbol{I}^{e}\cdot\left[\frac{\beta}{\gamma}\boldsymbol{K}^{-1}\cdot\boldsymbol{F}_{\beta}+\boldsymbol{K}^{-1}\cdot\boldsymbol{F}_{\gamma}\right].$$

After some algebra, the following results are obtained:

$$\begin{aligned}
\Xi_1^{(1)} &= B_1+\frac{\gamma}{\beta}B_2, \quad \Xi_3^{(1)}=\frac{\beta}{\gamma}B_3+B_4, \\
B_1 &= 2\frac{e_{0_{15}}\left[e_{1_{15}}+e_{0_{15}}\right]+\mu_0^{\mathrm{ax}}\left[\kappa_{1_{11}}+\kappa_{0_{11}}\right]}{\left[e_{1_{15}}+e_{0_{15}}\right]^2+\left[\kappa_{1_{11}}+\kappa_{0_{11}}\right]\left[\mu_1^{\mathrm{ax}}+\mu_0^{\mathrm{ax}}\right]}, \quad B_2=2\frac{e_{1_{15}}\kappa_{0_{11}}-e_{0_{15}}\kappa_{1_{11}}}{\left[e_{1_{15}}+e_{0_{15}}\right]^2+\left[\kappa_{1_{11}}+\kappa_{0_{11}}\right]\left[\mu_1^{\mathrm{ax}}+\mu_0^{\mathrm{ax}}\right]}, \\
B_3 &= 2\frac{e_{0_{15}}\mu_1^{\mathrm{ax}}-e_{1_{15}}\mu_0^{\mathrm{ax}}}{\left[e_{1_{15}}+e_{0_{15}}\right]^2+\left[\kappa_{1_{11}}+\kappa_{0_{11}}\right]\left[\mu_1^{\mathrm{ax}}+\mu_0^{\mathrm{ax}}\right]}, \quad B_4=2\frac{e_{0_{15}}\left[e_{1_{15}}+e_{0_{15}}\right]+\kappa_{0_{11}}\left[\mu_1^{\mathrm{ax}}+\mu_0^{\mathrm{ax}}\right]}{\left[e_{1_{15}}+e_{0_{15}}\right]^2+\left[\kappa_{1_{11}}+\kappa_{0_{11}}\right]\left[\mu_1^{\mathrm{ax}}+\mu_0^{\mathrm{ax}}\right]}.
\end{aligned}$$

Implementing the transformations (25), (26) and (27) in (23) yields the average strain and electric field inside the fiber,

$$\boldsymbol{\varepsilon}_1 = U_z^{(1)}(r_1)\,\boldsymbol{\varepsilon}_0 \qquad \rightarrow \qquad \boldsymbol{\varepsilon}_1 = B_1 \begin{bmatrix} 0 & 0 & \beta/2 \\ 0 & 0 & 0 \\ \beta/2 & 0 & 0 \end{bmatrix} + B_2 \begin{bmatrix} 0 & 0 & \gamma/2 \\ 0 & 0 & 0 \\ \gamma/2 & 0 & 0 \end{bmatrix},$$

$$\boldsymbol{E}_1 = \Phi^{(1)}(r_1)\,\boldsymbol{E}_0 \qquad \rightarrow \qquad \boldsymbol{E}_1 = B_3 \begin{bmatrix} \beta \\ 0 \\ 0 \end{bmatrix} + B_4 \begin{bmatrix} \gamma \\ 0 \\ 0 \end{bmatrix}.$$

Comparing these results with the expressions (22) and (28) it becomes clear that

$$\begin{aligned}
T_{1_{55}}^{mm} &= \left.\frac{\varepsilon_{1_{xz}}}{\beta/2}\right|_{\gamma=0} = B_1 = 2\frac{e_{0_{15}}\left[e_{1_{15}}+e_{0_{15}}\right]+\mu_0^{\mathrm{ax}}\left[\kappa_{1_{11}}+\kappa_{0_{11}}\right]}{\left[e_{1_{15}}+e_{0_{15}}\right]^2+\left[\kappa_{1_{11}}+\kappa_{0_{11}}\right]\left[\mu_1^{\mathrm{ax}}+\mu_0^{\mathrm{ax}}\right]}, \\
T_{1_{15}}^{me} &= \left.\frac{\varepsilon_{1_{xz}}}{\gamma/2}\right|_{\beta=0} = B_2 = 2\frac{e_{1_{15}}\kappa_{0_{11}}-e_{0_{15}}\kappa_{1_{11}}}{\left[e_{1_{15}}+e_{0_{15}}\right]^2+\left[\kappa_{1_{11}}+\kappa_{0_{11}}\right]\left[\mu_1^{\mathrm{ax}}+\mu_0^{\mathrm{ax}}\right]}, \\
T_{1_{15}}^{em} &= \left.\frac{E_{1_x}}{\beta}\right|_{\gamma=0} = B_3 = 2\frac{e_{0_{15}}\mu_1^{\mathrm{ax}}-e_{1_{15}}\mu_0^{\mathrm{ax}}}{\left[e_{1_{15}}+e_{0_{15}}\right]^2+\left[\kappa_{1_{11}}+\kappa_{0_{11}}\right]\left[\mu_1^{\mathrm{ax}}+\mu_0^{\mathrm{ax}}\right]}, \\
T_{1_{11}}^{ee} &= \left.\frac{E_{1_x}}{\gamma}\right|_{\beta=0} = B_4 = 2\frac{e_{0_{15}}\left[e_{1_{15}}+e_{0_{15}}\right]+\kappa_{0_{11}}\left[\mu_1^{\mathrm{ax}}+\mu_0^{\mathrm{ax}}\right]}{\left[e_{1_{15}}+e_{0_{15}}\right]^2+\left[\kappa_{1_{11}}+\kappa_{0_{11}}\right]\left[\mu_1^{\mathrm{ax}}+\mu_0^{\mathrm{ax}}\right]}.
\end{aligned} \tag{32}$$

3.2. Transverse shear strain conditions

For this case the following displacement vector is applied:

$$\boldsymbol{u}_0^{(x,y,z)} = \begin{bmatrix} \beta y \\ \beta x \\ 0 \end{bmatrix}, \tag{33}$$

which corresponds to the strain tensor (in classical tensorial form)

$$\boldsymbol{\varepsilon}_0 = \begin{bmatrix} 0 & \beta & 0 \\ \beta & 0 & 0 \\ 0 & 0 & 0 \end{bmatrix}.$$

In cylindrical coordinates, the displacement is transformed to the vector

$$\boldsymbol{u}_0^{(r,\theta,z)} = \begin{bmatrix} \beta r \sin 2\theta \\ \beta r \cos 2\theta \\ 0 \end{bmatrix}.$$

For these boundary conditions, the displacements at each phase are given by the general expressions

$$\begin{aligned}
u_r^{(q)}(r,\theta) &= \beta\, r\, U_r^{(q)}(r)\, \sin 2\theta\,, \\
u_\theta^{(q)}(r,\theta) &= \beta\, r\, U_\theta^{(q)}(r)\, \cos 2\theta\,, \\
U_r^{(q)}(r) &= \frac{K_q^{\rm tr} - \mu_q^{\rm tr}}{2K_q^{\rm tr} + \mu_q^{\rm tr}}[r/r_1]^2 \Xi_1^{(q)} + \Xi_2^{(q)} - \frac{1}{[r/r_1]^4}\Xi_3^{(q)} + \frac{K_q^{\rm tr} + \mu_q^{\rm tr}}{\mu_q^{\rm tr}}\frac{1}{[r/r_1]^2}\Xi_4^{(q)}\,, \\
U_\theta^{(q)}(r) &= [r/r_1]^2 \Xi_1^{(q)} + \Xi_2^{(q)} + \frac{1}{[r/r_1]^4}\Xi_3^{(q)} + \frac{1}{[r/r_1]^2}\Xi_4^{(q)}\,,
\end{aligned} \tag{34}$$

where the unknowns that need to be defined are the $\Xi_i^{(q)}$, $i = 1, 2, 3, 4$. These expressions lead to stresses and electric displacements that satisfy the equilibrium and electrostatic equations (19). The important stresses for the calculations are given by

$$\begin{aligned}
\sigma_{rr}^{(q)}(r,\theta) &= \beta\, \Sigma_{rr}^{(q)}(r) \sin 2\theta\,, \\
\sigma_{r\theta}^{(q)}(r,\theta) &= \beta\, \Sigma_{r\theta}^{(q)}(r) \cos 2\theta\,, \\
\Sigma_{rr}^{(q)}(r) &= 2\mu_q^{\rm tr}\Xi_2^{(q)} + 6\mu_q^{\rm tr}\frac{1}{[r/r_1]^4}\Xi_3^{(q)} - 4K_q^{\rm tr}\frac{1}{[r/r_1]^2}\Xi_4^{(q)}\,, \\
\Sigma_{r\theta}^{(q)}(r) &= \frac{6K_q^{\rm tr}\mu_q^{\rm tr}}{2K_q^{\rm tr} + \mu_q^{\rm tr}}[r/r_1]^2\Xi_1^{(q)} + 2\mu_q^{\rm tr}\Xi_2^{(q)} - 6\mu_q^{\rm tr}\frac{1}{[r/r_1]^4}\Xi_3^{(q)} + 2K_q^{\rm tr}\frac{1}{[r/r_1]^2}\Xi_4^{(q)}\,.
\end{aligned}$$

The boundary conditions that should be satisfied in this boundary value problem are

$$\begin{aligned}
u_r^{(1)}, u_\theta^{(1)} \text{ finite at } r = 0 \quad &\rightarrow \quad \Xi_3^{(1)} = \Xi_4^{(1)} = 0\,, \\
u_r^{(0)}(r \to \infty, \theta) = \beta r \sin 2\theta \;\text{ and }\; u_\theta^{(0)}(r \to \infty, \theta) = \beta r \cos 2\theta \quad &\rightarrow \quad \Xi_1^{(0)} = 0,\;\; \Xi_2^{(0)} = 1\,.
\end{aligned} \tag{35}$$

Considering these results, the interface conditions

$$u_r^{(1)}(r_1,\theta) = u_r^{(0)}(r_1,\theta), \quad u_\theta^{(1)}(r_1,\theta) = u_\theta^{(0)}(r_1,\theta), \quad \sigma_{rr}^{(1)}(r_1,\theta) = \sigma_{rr}^{(0)}(r_1,\theta), \quad \sigma_{r\theta}^{(1)}(r_1,\theta) = \sigma_{r\theta}^{(0)}(r_1,\theta),$$

construct the linear system

$$\boldsymbol{K}\cdot\boldsymbol{\Xi} = \boldsymbol{F},$$

with

$$\boldsymbol{K} = \begin{bmatrix} \dfrac{K_1^{\mathrm{tr}} - \mu_1^{\mathrm{tr}}}{2K_1^{\mathrm{tr}} + \mu_1^{\mathrm{tr}}} & 1 & 1 & -\dfrac{K_0^{\mathrm{tr}} + \mu_0^{\mathrm{tr}}}{\mu_0^{\mathrm{tr}}} \\ 1 & 1 & -1 & -1 \\ 0 & 2\mu_1^{\mathrm{tr}} & -6\mu_0^{\mathrm{tr}} & 4K_0^{\mathrm{tr}} \\ \dfrac{6K_1^{\mathrm{tr}}\mu_1^{\mathrm{tr}}}{2K_1^{\mathrm{tr}} + \mu_1^{\mathrm{tr}}} & 2\mu_1^{\mathrm{tr}} & 6\mu_0^{\mathrm{tr}} & -2K_0^{\mathrm{tr}} \end{bmatrix}, \quad \boldsymbol{\Xi} = \begin{bmatrix} \Xi_1^{(1)} \\ \Xi_2^{(1)} \\ \Xi_3^{(0)} \\ \Xi_4^{(0)} \end{bmatrix}, \quad \boldsymbol{F} = \begin{bmatrix} 1 \\ 1 \\ 2\mu_0^{\mathrm{tr}} \\ 2\mu_0^{\mathrm{tr}} \end{bmatrix}.$$

The solution of this linear system gives

$$\Xi_1^{(1)} = 0, \qquad \Xi_2^{(1)} = \frac{2\mu_0^{\mathrm{tr}}\left[K_0^{\mathrm{tr}} + \mu_0^{\mathrm{tr}}\right]}{2\mu_0^{\mathrm{tr}}\mu_1^{\mathrm{tr}} + K_0^{\mathrm{tr}}\left[\mu_1^{\mathrm{tr}} + \mu_0^{\mathrm{tr}}\right]}.$$

Implementing the transformations (25), (26) and (27) in (23) yields the average strain inside the fiber,

$$\boldsymbol{\varepsilon}_1 = \frac{1}{2}\left[U_r^{(1)}(r_1) + U_\theta^{(1)}(r_1)\right]\boldsymbol{\varepsilon}_0 \quad \rightarrow \quad \boldsymbol{\varepsilon}_1 = \Xi_2^{(1)}\,\boldsymbol{\varepsilon}_0\,.$$

Comparing these results with the expressions (22) and (28) it becomes clear that

$$T_{1_{44}}^{mm} = \frac{\varepsilon_{1_{xy}}}{\beta} = \Xi_2^{(1)} = \frac{2\mu_0^{\mathrm{tr}}\left[K_0^{\mathrm{tr}} + \mu_0^{\mathrm{tr}}\right]}{2\mu_0^{\mathrm{tr}}\mu_1^{\mathrm{tr}} + K_0^{\mathrm{tr}}\left[\mu_1^{\mathrm{tr}} + \mu_0^{\mathrm{tr}}\right]}. \tag{36}$$

3.3. Plane strain and axial electric field conditions

For this case the following displacement vector and electric potential are applied:

$$\boldsymbol{u}_0^{(x,y,z)} = \begin{bmatrix} \beta x \\ \beta y \\ 0 \end{bmatrix}, \qquad \phi_0^{(x,y,z)} = -\gamma z. \tag{37}$$

These correspond to the following strain tensor (in classical tensorial form) and electric field vector

$$\boldsymbol{\varepsilon}_0 = \begin{bmatrix} \beta & 0 & 0 \\ 0 & \beta & 0 \\ 0 & 0 & 0 \end{bmatrix}, \qquad \boldsymbol{E}_0 = \begin{bmatrix} 0 \\ 0 \\ \gamma \end{bmatrix}.$$

In cylindrical coordinates, the displacement and electric potential are transformed to

$$\boldsymbol{u}_0^{(r,\theta,z)} = \begin{bmatrix} \beta r \\ 0 \\ 0 \end{bmatrix}, \qquad \phi_0^{(r,\theta,z)} = -\gamma z.$$

For these boundary conditions, the displacement vector and electric potential at the matrix ($q = 0$) and the fiber ($q = 1$) are given by the general expressions

$$\begin{aligned} u_r^{(q)}(r) &= \beta r U_r^{(q)}(r), \quad u_\theta^{(q)} = u_z^{(q)} = 0, \quad U_r^{(q)}(r) = \Xi_1^{(q)} + \Xi_2^{(q)} \frac{1}{[r/r_1]^2}, \\ \phi^{(q)}(z) &= -\gamma z, \end{aligned} \tag{38}$$

where $\Xi_i^{(q)}$, $i = 1, 2$, are unknown constants. These general expressions lead to stresses and electric displacements that satisfy the equilibrium and electrostatic equations (19). The important stresses for identifying the unknown constants are

$$\sigma_{rr}^{(q)}(r) = \beta\, \Sigma_{rr}^{m(q)}(r) + \gamma\, \Sigma_{rr}^{e(q)}, \quad \Sigma_{rr}^{m(q)}(r) = 2\left[K_q^{\mathrm{tr}} \Xi_1^{(q)} - \mu_q^{\mathrm{tr}} \Xi_2^{(q)} \frac{1}{[r/r_1]^2}\right], \quad \Sigma_{rr}^{e(q)} = -e_{31}^{(q)}\,.$$

The boundary conditions that should be satisfied in this boundary value problem are

$$\begin{aligned} u_r^{(1)} \text{ finite at } r = 0 \quad &\rightarrow \quad D_2^{(1)} = 0\,, \\ u_r^{(0)}(r \rightarrow \infty) = \beta r \quad &\rightarrow \quad D_1^{(0)} = 1\,. \end{aligned} \tag{39}$$

Considering these results, the interface conditions

$$u_r^{(1)}(r_1) = u_r^{(0)}(r_1), \quad \sigma_{rr}^{(1)}(r_1) = \sigma_{rr}^{(0)}(r_1),$$

construct the linear system

$$\boldsymbol{K} \cdot \boldsymbol{\Xi} = \boldsymbol{F}_\beta + \frac{\gamma}{\beta}\, \boldsymbol{F}_\gamma,$$

with

$$\boldsymbol{K} = \begin{bmatrix} 1 & -1 \\ 2K_1^{\mathrm{tr}} & 2\mu_0^{\mathrm{tr}} \end{bmatrix}, \quad \boldsymbol{\Xi} = \begin{bmatrix} \Xi_1^{(1)} \\ \Xi_2^{(0)} \end{bmatrix}, \quad \boldsymbol{F}_\beta = \begin{bmatrix} 1 \\ 2K_0^{\mathrm{tr}} \end{bmatrix}, \quad \boldsymbol{F}_\gamma = \begin{bmatrix} 0 \\ e_{1_{31}} - e_{0_{31}} \end{bmatrix}.$$

The solution of this linear system gives

$$\Xi_1^{(1)} = B_1 + \frac{\gamma}{\beta} B_2, \qquad B_1 = \frac{K_0^{\mathrm{tr}} + \mu_0^{\mathrm{tr}}}{K_1^{\mathrm{tr}} + \mu_0^{\mathrm{tr}}}, \quad B_2 = \frac{e_{1_{31}} - e_{0_{31}}}{2K_1^{\mathrm{tr}} + 2\mu_0^{\mathrm{tr}}}. \tag{40}$$

Implementing the transformations (25), (26) and (27) in (23) yields the average strain inside the fiber,

$$\boldsymbol{\varepsilon}_1 = U_r^{(1)}(r_1)\, \boldsymbol{\varepsilon}_0 \quad \rightarrow \quad \boldsymbol{\varepsilon}_1 = B_1 \begin{bmatrix} \beta & 0 & 0 \\ 0 & \beta & 0 \\ 0 & 0 & 0 \end{bmatrix} + B_2 \begin{bmatrix} \gamma & 0 & 0 \\ 0 & \gamma & 0 \\ 0 & 0 & 0 \end{bmatrix}. \tag{41}$$

The general form of the dilute concentration tensors (22) and (28) permits to write

$$\varepsilon_{1_{xx}} = [2T_{1_{11}}^{mm} - T_{1_{44}}^{mm}]\,\beta + T_{1_{31}}^{me}\,\gamma.$$

From (40) and (41), it becomes clear that

$$T_{1_{11}}^{mm} = \frac{1}{2}\left[\frac{K_0^{\mathrm{tr}} + \mu_0^{\mathrm{tr}}}{K_1^{\mathrm{tr}} + \mu_0^{\mathrm{tr}}} + T_{1_{44}}^{mm}\right], \quad T_{1_{31}}^{me} = \frac{e_{1_{31}} - e_{0_{31}}}{2K_1^{\mathrm{tr}} + 2\mu_0^{\mathrm{tr}}}. \tag{42}$$

3.4. Hydrostatic strain conditions

For this case the following displacement vector is applied:

$$\boldsymbol{u}_0^{(x,y,z)} = \begin{bmatrix} \beta x \\ \beta y \\ \beta z \end{bmatrix}, \tag{43}$$

which corresponds to the strain tensor (in classical tensorial form)

$$\boldsymbol{\varepsilon}_0 = \begin{bmatrix} \beta & 0 & 0 \\ 0 & \beta & 0 \\ 0 & 0 & \beta \end{bmatrix}.$$

In cylindrical coordinates, the displacement is transformed to the vector

$$\boldsymbol{u}_0^{(r,\theta,z)} = \begin{bmatrix} \beta r \\ 0 \\ \beta z \end{bmatrix}.$$

For these boundary conditions, the displacement vector and electric potential at the matrix ($q = 0$) and the fiber ($q = 1$) are given by the general expressions

$$u_r^{(q)}(r) = \beta r U_r^{(q)}(r), \quad u_\theta^{(q)} = 0, \quad u_z^{(q)}(z) = \beta z, \qquad U_r^{(q)}(r) = \Xi_1^{(q)} + \Xi_2^{(q)} \frac{1}{[r/r_1]^2}, \tag{44}$$

where $\Xi_i^{(q)}$, $i = 1, 2$, are unknown constants. These general expressions lead to stresses and electric displacements that satisfy the equilibrium and electrostatic equations (19). The important stresses for identifying the unknown constants are

$$\sigma_{rr}^{(q)}(r) = \beta\, \Sigma_{rr}^{(q)}(r), \quad \Sigma_{rr}^{(q)}(r) = 2\left[K_q^{\mathrm{tr}} \Xi_1^{(q)} - \mu_q^{\mathrm{tr}} \Xi_2^{(q)} \frac{1}{[r/r_1]^2}\right] + l_q\,.$$

The boundary conditions that should be satisfied in this boundary value problem are

$$\begin{aligned} u_r^{(1)} \text{ finite at } r = 0 \quad &\rightarrow \quad D_2^{(1)} = 0\,, \\ u_r^{(0)}(r \rightarrow \infty) = \beta r \quad &\rightarrow \quad D_1^{(0)} = 1\,. \end{aligned} \tag{45}$$

Considering these results, the interface conditions

$$u_r^{(1)}(r_1) = u_r^{(0)}(r_1), \quad \sigma_{rr}^{(1)}(r_1) = \sigma_{rr}^{(0)}(r_1),$$

construct the linear system

$$\boldsymbol{K} \cdot \boldsymbol{\Xi} = \boldsymbol{F},$$

with

$$\boldsymbol{K} = \begin{bmatrix} 1 & -1 \\ 2K_1^{\mathrm{tr}} & 2\mu_0^{\mathrm{tr}} \end{bmatrix}, \quad \boldsymbol{\Xi} = \begin{bmatrix} \Xi_1^{(1)} \\ \Xi_2^{(0)} \end{bmatrix}, \quad \boldsymbol{F} = \begin{bmatrix} 1 \\ 2K_0^{\mathrm{tr}} + l_0 - l_1 \end{bmatrix}.$$

The solution of this linear system gives

$$\Xi_1^{(1)} = \frac{K_0^{\mathrm{tr}} + \mu_0^{\mathrm{tr}}}{K_1^{\mathrm{tr}} + \mu_0^{\mathrm{tr}}} + \frac{l_0 - l_1}{2K_1^{\mathrm{tr}} + 2\mu_0^{\mathrm{tr}}}. \tag{46}$$

Implementing the transformations (25), (26) and (27) in (23) yields the average strain inside the fiber,

$$\boldsymbol{\varepsilon}_1 = U_r^{(1)}(r_1)\, \boldsymbol{\varepsilon}_0 \quad \rightarrow \quad \boldsymbol{\varepsilon}_1 = \Xi_1^{(1)} \boldsymbol{\varepsilon}_0. \tag{47}$$

The general form of the dilute concentration tensors (22) and (28) permits to write

$$\varepsilon_{1_{xx}} = [2T^{mm}_{1_{11}} - T^{mm}_{1_{44}} + T^{mm}_{1_{13}}]\, \beta.$$

From (46), (47) and (42), it becomes clear that

$$T^{mm}_{1_{13}} = \frac{l_0 - l_1}{2K_1^{\mathrm{tr}} + 2\mu_0^{\mathrm{tr}}}. \tag{48}$$

3.5. Macroscopic properties

The dilute concentration tensors (28), whose terms are given by (32), (36), (42) and (48), are equivalent to the global piezoelectric concentration tensor provided by Dunn and Taya (1993) (see Appendix A). Assuming that the volume fraction of fibers in the composite is c and applying the Mori-Tanaka scheme, as described in subsection 2.2, the following macroscopic properties are obtained:

$$\bar{K}^{\mathrm{tr}} = \frac{cK_1^{\mathrm{tr}}\mu_0^{\mathrm{tr}} + K_0^{\mathrm{tr}}\left[K_1^{\mathrm{tr}} + \mu_0^{\mathrm{tr}} - c\mu_0^{\mathrm{tr}}\right]}{cK_0^{\mathrm{tr}} - cK_1^{\mathrm{tr}} + K_1^{\mathrm{tr}} + \mu_0^{\mathrm{tr}}}, \quad \bar{\mu}^{\mathrm{tr}} = \frac{\mu_0^{\mathrm{tr}}\left[2\mu_0^{\mathrm{tr}}\mu_1^{\mathrm{tr}} + K_0^{\mathrm{tr}}\left[\mu_0^{\mathrm{tr}} - c\mu_0^{\mathrm{tr}} + \mu_1^{\mathrm{tr}} + c\mu_1^{\mathrm{tr}}\right]\right]}{2\mu_0^{\mathrm{tr}}\left[c\mu_0^{\mathrm{tr}} - c\mu_1^{\mathrm{tr}} + \mu_1^{\mathrm{tr}}\right] + K_0^{\mathrm{tr}}\left[\mu_0^{\mathrm{tr}} + c\mu_0^{\mathrm{tr}} + \mu_1^{\mathrm{tr}} - c\mu_1^{\mathrm{tr}}\right]},$$

$$\bar{l} = \frac{[1-c]\left[K_1^{\mathrm{tr}} + \mu_0^{\mathrm{tr}}\right] l_0 + c\left[K_0^{\mathrm{tr}} + \mu_0^{\mathrm{tr}}\right] l_1}{cK_0^{\mathrm{tr}} - cK_1^{\mathrm{tr}} + K_1^{\mathrm{tr}} + \mu_0^{\mathrm{tr}}}, \quad \bar{n} = \frac{Z_1}{cK_0^{\mathrm{tr}} - cK_1^{\mathrm{tr}} + K_1^{\mathrm{tr}} + \mu_0^{\mathrm{tr}}}, \quad \bar{\mu}^{\mathrm{ax}} = \frac{W_2}{W_1},$$

$$\bar{e}_{31} = \frac{ce_{1_{31}}\left[K_0^{\mathrm{tr}} + \mu_0^{\mathrm{tr}}\right] + [1-c]e_{0_{31}}\left[K_1^{\mathrm{tr}} + \mu_0^{\mathrm{tr}}\right]}{cK_0^{\mathrm{tr}} - cK_1^{\mathrm{tr}} + K_1^{\mathrm{tr}} + \mu_0^{\mathrm{tr}}}, \quad \bar{e}_{33} = \frac{Z_2}{cK_0^{\mathrm{tr}} - cK_1^{\mathrm{tr}} + K_1^{\mathrm{tr}} + \mu_0^{\mathrm{tr}}}, \quad \bar{e}_{15} = \frac{W_3}{W_1},$$

$$\bar{\kappa}_{11} = \frac{W_4}{W_1}, \quad \bar{\kappa}_{33} = \frac{Z_3}{cK_0^{\mathrm{tr}} - cK_1^{\mathrm{tr}} + K_1^{\mathrm{tr}} + \mu_0^{\mathrm{tr}}},$$

where

$$
\begin{aligned}
Z_1 &= c^2\left[[l_0-l_1]^2-\left[K_0^{\rm tr}-K_1^{\rm tr}\right][n_0-n_1]\right]+[n_0-cn_0+cn_1]\left[K_1^{\rm tr}+\mu_0^{\rm tr}\right]\\
&\quad -c\left[[l_0-l_1]^2+n_0\left[K_1^{\rm tr}-K_0^{\rm tr}\right]\right],\\
Z_2 &= c^2\left[\left[K_0^{\rm tr}-K_1^{\rm tr}\right][e_{1_{33}}-e_{0_{33}}]+[l_0-l_1]\left[e_{0_{31}}-e_{1_{31}}\right]\right]+\left[e_{0_{33}}-ce_{0_{33}}+ce_{1_{33}}\right]\left[K_1^{\rm tr}+\mu_0^{\rm tr}\right]\\
&\quad +c\left[[l_0-l_1]\left[e_{1_{31}}-e_{0_{31}}\right]+e_{0_{33}}\left[K_0^{\rm tr}-\mu_0^{\rm tr}\right]\right],\\
Z_3 &= -c^2\left[\left[e_{0_{31}}-e_{1_{31}}\right]^2+\left[K_0^{\rm tr}-K_1^{\rm tr}\right]\left[\kappa_{0_{33}}-\kappa_{1_{33}}\right]\right]+\left[\kappa_{0_{33}}-c\kappa_{0_{33}}+c\kappa_{1_{33}}\right]\left[K_1^{\rm tr}+\mu_0^{\rm tr}\right]\\
&\quad +c\left[\left[e_{0_{31}}-e_{1_{31}}\right]^2+\kappa_{0_{33}}\left[K_0^{\rm tr}-K_1^{\rm tr}\right]\right],
\end{aligned}
$$

$$
\begin{aligned}
W_1 &= [1+c]^2[e_{0_{15}}]^2+2[1-c^2]e_{0_{15}}e_{1_{15}}+[1-c]^2[e_{1_{15}}]^2\\
&\quad +\left[\kappa_{0_{11}}+c\kappa_{0_{11}}+\kappa_{1_{11}}-c\kappa_{1_{11}}\right]\left[\mu_0^{\rm ax}+c\mu_0^{\rm ax}+\mu_1^{\rm ax}-c\mu_1^{\rm ax}\right],\\
W_2 &= 2[1-c]^2e_{0_{15}}e_{1_{15}}\mu_0^{\rm ax}+[1-c^2]\left[[e_{1_{15}}]^2+[e_{0_{15}}]^2\right]\mu_0^{\rm ax}+4c[e_{0_{15}}]^2\mu_1^{\rm ax}\\
&\quad +\left[\kappa_{0_{11}}+c\kappa_{0_{11}}+\kappa_{1_{11}}-c\kappa_{1_{11}}\right]\left[\mu_0^{\rm ax}-c\mu_0^{\rm ax}+\mu_1^{\rm ax}+c\mu_1^{\rm ax}\right]\mu_0^{\rm ax},\\
W_3 &= [1-c^2]\left[[e_{0_{15}}]^3+[e_{1_{15}}]^2e_{0_{15}}\right]+\left[2[1+c]^2[e_{0_{15}}]^2+4c\kappa_{0_{11}}\mu_0^{\rm ax}\right]e_{1_{15}}\\
&\quad +[1-c]\left[\kappa_{0_{11}}\left[\mu_0^{\rm ax}+c\mu_0^{\rm ax}+\mu_1^{\rm ax}-c\mu_1^{\rm ax}\right]+\kappa_{1_{11}}\left[\mu_0^{\rm ax}-c\mu_0^{\rm ax}+\mu_1^{\rm ax}+c\mu_1^{\rm ax}\right]\right]e_{0_{15}},\\
W_4 &= 2[1-c]^2e_{0_{15}}e_{1_{15}}\kappa_{0_{11}}+[1-c^2]\left[[e_{1_{15}}]^2+[e_{0_{15}}]^2\right]\kappa_{0_{11}}+4c[e_{0_{15}}]^2\kappa_{1_{11}}\\
&\quad +\left[\kappa_{0_{11}}-c\kappa_{0_{11}}+\kappa_{1_{11}}+c\kappa_{1_{11}}\right]\left[\mu_0^{\rm ax}+c\mu_0^{\rm ax}+\mu_1^{\rm ax}-c\mu_1^{\rm ax}\right]\kappa_{0_{11}}.
\end{aligned}
$$

The obtained solution respects the compatibility condition between equations $(14)_2$ and $(14)_3$. The above properties agree with the findings of Benveniste (1994). The transverse bulk modulus $\overline{K}^{\rm tr}$ is given by the same expression, while for the transverse shear modulus $\bar{\mu}^{\rm tr}$, Benveniste also concluded that it depends exclusively on the mechanical properties. For calculating $\bar{\mu}^{\rm tr}$ he proposed the use of the Christensen and Lo (1979) approach, which is a generalized self consistent method and provides quite similar results with Mori-Tanaka. The rest of the properties satisfy the universal relations (Benveniste and Dvorak, 1992)

$$
\begin{aligned}
\frac{K_0^{\rm tr}-\overline{K}^{\rm tr}}{l_0-\bar{l}}&=\frac{K_1^{\rm tr}-\overline{K}^{\rm tr}}{l_1-\bar{l}}=\frac{cl_1+[1-c]l_0-\bar{l}}{cn^{(1)}+[1-c]n^{(0)}-\bar{n}}=\frac{ce_{1_{31}}+[1-c]e_{0_{31}}-\bar{e}_{31}}{ce_{33}^{(1)}+[1-c]e_{33}^{(0)}-\bar{e}_{33}},\\
\frac{K_0^{\rm tr}-\overline{K}^{\rm tr}}{e_{0_{31}}-\bar{e}_{31}}&=\frac{K_1^{\rm tr}-\overline{K}^{\rm tr}}{e_{1_{31}}-\bar{e}_{31}}=\frac{cl_1+[1-c]l_0-\bar{l}}{ce_{33}^{(1)}+[1-c]e_{33}^{(0)}-\bar{e}_{33}}=\frac{\bar{e}_{31}-ce_{1_{31}}-[1-c]e_{0_{31}}}{c\kappa_{1_{33}}+[1-c]\kappa_{0_{33}}-\bar{\kappa}_{33}},
\end{aligned}
$$

and

$$\mathrm{Det}\begin{bmatrix} \bar{\mu}^{\mathrm{ax}} & \bar{e}_{15} & -\bar{\kappa}_{11} \\ \mu_1^{\mathrm{ax}} & e_{1_{15}} & -\kappa_{1_{11}} \\ \mu_0^{\mathrm{ax}} & e_{0_{15}} & -\kappa_{0_{11}} \end{bmatrix} = 0.$$

There are two main advantages of the proposed methodology compared to that of Benveniste (1994): a) The computation of the strain and electric field concentration tensors allow the identification of the microscopic electromechanical fields for known macroscopic fields. Such information can be very valuable for detecting possible inelastic mechanisms due to high stresses in the matrix or the fiber. b) The dilute concentration tensors can be used into the Mori-Tanaka scheme for obtaining the macroscopic response of composites with more complex microstructure, for instance with two different types of fibers, or the same fibers with random orientation (Chatzigeorgiou et al., 2012; Seidel et al., 2014).

4. Second case: fibers with one coating layer

In this second studied case, the composite consists of coated fibers and matrix. Each fiber has radius $r = r_1$ and is coated with a layer that has external radius $r = r_2$. In the sequel, the ratio $\rho = r_1/r_2$ will be utilized. Considering as c the volume fraction of the fibers, the coating layers and the matrix volume fraction can be computed through the ratio ρ. Indeed, the volume fractions of all the phases (fiber, coating, matrix) are

$$c_1 = c, \quad c_2 = \frac{c}{\rho^2} - c, \quad c_0 = 1 - c_1 - c_2 = 1 - \frac{c}{\rho^2}. \tag{49}$$

The dilute concentration tensors are computed with similar boundary value problems as those discussed in the previous section. Here, only the essential different points are going to be presented.

For the sake of the procedure's simplicity, only one coating layer is considered for this section. Nevertheless, the approach is general and the addition of more coating layers is straightforward.

4.1. Axial shear strain and in-plane electric field conditions

Similarly to the non-coated fibers, the infinite matrix is subjected to the far field displacement vector and electric potential of (29). For all phases (matrix, fiber, coating) the general expressions (30) for these fields introduce 12 unknowns (4 constants per phase). After eliminating four from the boundary conditions (31), the rest of the unknowns are identified from the interface conditions that hold between the fiber and the coating and between the coating and the matrix. The produced system of linear equations take the form

$$\boldsymbol{K}\cdot\left[\beta\,\boldsymbol{I}^{m}+\gamma\,\boldsymbol{I}^{e}\right]\cdot\left[\boldsymbol{\Xi}^{m}+\boldsymbol{\Xi}^{e}\right]=\beta\,\boldsymbol{F}_{\beta}+\gamma\,\boldsymbol{F}_{\gamma},$$

with

$$\boldsymbol{K}=\begin{bmatrix}
1 & -1 & -1 & 0 & 0 & 0 & 0 & 0\\
0 & 1 & \rho^2 & -\rho^2 & 0 & 0 & 0 & 0\\
\mu_1^{\mathrm{ax}} & -\mu_2^{\mathrm{ax}} & \mu_2^{\mathrm{ax}} & 0 & -e_{1_{15}} & e_{2_{15}} & -e_{2_{15}} & 0\\
0 & \mu_2^{\mathrm{ax}} & -\rho^2\mu_2^{\mathrm{ax}} & \rho^2\mu_0^{\mathrm{ax}} & 0 & -e_{2_{15}} & \rho^2 e_{2_{15}} & -\rho^2 e_{0_{15}}\\
0 & 0 & 0 & 0 & 1 & -1 & -1 & 0\\
0 & 0 & 0 & 0 & 0 & 1 & \rho^2 & -\rho^2\\
e_{1_{15}} & -e_{2_{15}} & e_{2_{15}} & 0 & \kappa_{1_{11}} & -\kappa_{2_{11}} & \kappa_{2_{11}} & 0\\
0 & e_{2_{15}} & -\rho^2 e_{2_{15}} & \rho^2 e_{0_{15}} & 0 & \kappa_{2_{11}} & -\rho^2\kappa_{2_{11}} & \rho^2\kappa_{0_{11}}
\end{bmatrix},$$

$$\boldsymbol{I}^m = \begin{bmatrix} 1&0&0&0&0&0&0&0\\ 0&1&0&0&0&0&0&0\\ 0&0&1&0&0&0&0&0\\ 0&0&0&1&0&0&0&0\\ 0&0&0&0&0&0&0&0\\ 0&0&0&0&0&0&0&0\\ 0&0&0&0&0&0&0&0\\ 0&0&0&0&0&0&0&0 \end{bmatrix}, \quad \boldsymbol{I}^e = \begin{bmatrix} 0&0&0&0&0&0&0&0\\ 0&0&0&0&0&0&0&0\\ 0&0&0&0&0&0&0&0\\ 0&0&0&0&0&0&0&0\\ 0&0&0&0&1&0&0&0\\ 0&0&0&0&0&1&0&0\\ 0&0&0&0&0&0&1&0\\ 0&0&0&0&0&0&0&1 \end{bmatrix},$$

$$\boldsymbol{\Xi}^m = \begin{bmatrix} \Xi_1^{(1)} & \Xi_1^{(2)} & \Xi_2^{(2)} & \Xi_2^{(0)} & 0 & 0 & 0 & 0 \end{bmatrix}^T, \quad \boldsymbol{\Xi}^e = \begin{bmatrix} 0 & 0 & 0 & 0 & \Xi_3^{(1)} & \Xi_3^{(2)} & \Xi_4^{(2)} & \Xi_4^{(0)} \end{bmatrix}^T,$$

$$\boldsymbol{F}_\beta = \begin{bmatrix} 0 & 1 & 0 & \mu_0^{\text{ax}} & 0 & 0 & 0 & e_{0_{15}} \end{bmatrix}^T, \quad \boldsymbol{F}_\gamma = \begin{bmatrix} 0 & 0 & 0 & -e_{0_{15}} & 0 & 1 & 0 & \kappa_{0_{11}} \end{bmatrix}^T.$$

The solution of this linear system is expressed as

$$\boldsymbol{\Xi}^m = \boldsymbol{I}^m \cdot \left[\boldsymbol{K}^{-1} \cdot \boldsymbol{F}_\beta + \frac{\gamma}{\beta} \boldsymbol{K}^{-1} \cdot \boldsymbol{F}_\gamma \right], \quad \boldsymbol{\Xi}^e = \boldsymbol{I}^e \cdot \left[\frac{\beta}{\gamma} \boldsymbol{K}^{-1} \cdot \boldsymbol{F}_\beta + \boldsymbol{K}^{-1} \cdot \boldsymbol{F}_\gamma \right].$$

Considering the dilute tensors, the important terms $\Xi_1^{(1)}$, $\Xi_3^{(1)}$, $\Xi_2^{(0)}$ and $\Xi_4^{(0)}$ can be written in the general form

$$\Xi_1^{(1)} = B_1 + \frac{\gamma}{\beta} B_2, \quad \Xi_3^{(1)} = \frac{\beta}{\gamma} B_3 + B_4, \quad \Xi_2^{(0)} = B_5 + \frac{\gamma}{\beta} B_6, \quad \Xi_4^{(0)} = \frac{\beta}{\gamma} B_7 + B_8.$$

Implementing the transformations (25), (26) and (27) in (23) yields the average strain and electric field inside the fiber,

$$\boldsymbol{\varepsilon}_1 = U_z^{(1)}(r_1)\, \boldsymbol{\varepsilon}_0 \quad \rightarrow \quad \boldsymbol{\varepsilon}_1 = B_1 \begin{bmatrix} 0&0&\beta/2\\ 0&0&0\\ \beta/2&0&0 \end{bmatrix} + B_2 \begin{bmatrix} 0&0&\gamma/2\\ 0&0&0\\ \gamma/2&0&0 \end{bmatrix},$$

$$\boldsymbol{E}_1 = \Phi^{(1)}(r_1)\, \boldsymbol{E}_0 \quad \rightarrow \quad \boldsymbol{E}_1 = B_3 \begin{bmatrix} \beta\\0\\0 \end{bmatrix} + B_4 \begin{bmatrix} \gamma\\0\\0 \end{bmatrix}.$$

On the other hand, implementing the transformations (25), (26) and (27) in (24) and taking into account the displacement and electric potential continuity conditions yields the average strain and

electric field inside the coating,

$$
\begin{aligned}
\boldsymbol{\varepsilon}_2 &= \left[\frac{1}{1-\rho^2}U_z^{(0)}(r_2) - \frac{\rho^2}{1-\rho^2}U_z^{(1)}(r_1)\right]\boldsymbol{\varepsilon}_0 \quad \rightarrow \\
\boldsymbol{\varepsilon}_2 &= \frac{1+\rho^2 B_5 - \rho^2 B_1}{1-\rho^2}\begin{bmatrix} 0 & 0 & \beta/2 \\ 0 & 0 & 0 \\ \beta/2 & 0 & 0 \end{bmatrix} + \frac{\rho^2 B_6 - \rho^2 B_2}{1-\rho^2}\begin{bmatrix} 0 & 0 & \gamma/2 \\ 0 & 0 & 0 \\ \gamma/2 & 0 & 0 \end{bmatrix}, \\
\boldsymbol{E}_2 &= \left[\frac{1}{1-\rho^2}\Phi^{(0)}(r_2) - \frac{\rho^2}{1-\rho^2}\Phi^{(1)}(r_1)\right]\boldsymbol{E}_0 \quad \rightarrow \\
\boldsymbol{E}_2 &= \frac{\rho^2 B_7 - \rho^2 B_3}{1-\rho^2}\begin{bmatrix} \beta \\ 0 \\ 0 \end{bmatrix} + \frac{1+\rho^2 B_8 - \rho^2 B_4}{1-\rho^2}\begin{bmatrix} \gamma \\ 0 \\ 0 \end{bmatrix}.
\end{aligned}
$$

Comparing these results with the expressions (22) and (28) it becomes clear that

$$
\begin{aligned}
T^{mm}_{1_{55}} &= B_1, \qquad T^{me}_{1_{15}} = B_2, \\
T^{em}_{1_{15}} &= B_3, \qquad T^{ee}_{1_{11}} = B_4, \\
T^{mm}_{2_{55}} &= \frac{1+\rho^2 B_5 - \rho^2 B_1}{1-\rho^2}, \qquad T^{me}_{2_{15}} = \frac{\rho^2 B_6 - \rho^2 B_2}{1-\rho^2}, \\
T^{em}_{2_{15}} &= \frac{\rho^2 B_7 - \rho^2 B_3}{1-\rho^2}, \qquad T^{ee}_{2_{11}} = \frac{1+\rho^2 B_8 - \rho^2 B_4}{1-\rho^2}.
\end{aligned} \tag{50}
$$

4.2. Transverse shear strain conditions

For the transverse shear term of the dilute concentration tensor, the infinite matrix is subjected to the far field displacement vector of (33). For all phases (matrix, fiber, coating) the general expressions (34) introduce 12 unknowns (4 constants per phase). After eliminating four from the boundary conditions (35), the rest of the unknowns are identified from the interface conditions that hold between the fiber and the coating and between the coating and the matrix. The produced system of linear equations take the form

$$
\boldsymbol{K}\cdot\boldsymbol{\Xi} = \boldsymbol{F},
$$

with

$$\boldsymbol{K} = \begin{bmatrix} \frac{K_1^{\rm tr}-\mu_1^{\rm tr}}{2K_1^{\rm tr}+\mu_1^{\rm tr}} & 1 & -\frac{K_2^{\rm tr}-\mu_2^{\rm tr}}{2K_2^{\rm tr}+\mu_2^{\rm tr}} & -1 & 1 & -\frac{K_2^{\rm tr}+\mu_2^{\rm tr}}{\mu_2^{\rm tr}} & 0 & 0 \\ 1 & 1 & -1 & -1 & -1 & -1 & 0 & 0 \\ 0 & 0 & \frac{1}{\rho^2}\frac{K_2^{\rm tr}-\mu_2^{\rm tr}}{2K_2^{\rm tr}+\mu_2^{\rm tr}} & 1 & -\rho^4 & \rho^2\frac{K_2^{\rm tr}+\mu_2^{\rm tr}}{\mu_2^{\rm tr}} & \rho^4 & -\rho^2\frac{K_0^{\rm tr}+\mu_0^{\rm tr}}{\mu_0^{\rm tr}} \\ 0 & 0 & 1/\rho^2 & 1 & \rho^4 & \rho^2 & -\rho^4 & -\rho^2 \\ 0 & 2\mu_1^{\rm tr} & 0 & -2\mu_2^{\rm tr} & -6\mu_2^{\rm tr} & 4K_2^{\rm tr} & 0 & 0 \\ \frac{6K_1^{\rm tr}\mu_1^{\rm tr}}{2K_1^{\rm tr}+\mu_1^{\rm tr}} & 2\mu_1^{\rm tr} & -\frac{6K_2^{\rm tr}\mu_2^{\rm tr}}{2K_2^{\rm tr}+\mu_2^{\rm tr}} & -2\mu_2^{\rm tr} & 6\mu_2^{\rm tr} & -2K_2^{\rm tr} & 0 & 0 \\ 0 & 0 & 0 & 2\mu_2^{\rm tr} & 6\rho^4\mu_2^{\rm tr} & -4\rho^2K_2^{\rm tr} & -6\rho^4\mu_0^{\rm tr} & 4\rho^2K_0^{\rm tr} \\ 0 & 0 & \frac{1}{\rho^2}\frac{6K_2^{\rm tr}\mu_2^{\rm tr}}{2K_2^{\rm tr}+\mu_2^{\rm tr}} & 2\mu_2^{\rm tr} & -6\rho^4\mu_2^{\rm tr} & 2\rho^2K_2^{\rm tr} & 6\rho^4\mu_0^{\rm tr} & -2\rho^2K_0^{\rm tr} \end{bmatrix},$$

$$\boldsymbol{\Xi} = \begin{bmatrix} \Xi_1^{(1)} & \Xi_2^{(1)} & \Xi_1^{(2)} & \Xi_2^{(2)} & \Xi_3^{(2)} & \Xi_4^{(2)} & \Xi_3^{(0)} & \Xi_4^{(0)} \end{bmatrix}^T, \quad \boldsymbol{F} = \begin{bmatrix} 0 & 0 & 1 & 1 & 0 & 0 & 2\mu_0^{\rm tr} & 2\mu_0^{\rm tr} \end{bmatrix}^T.$$

The solution of this linear system is expressed as

$$\boldsymbol{\Xi} = \boldsymbol{K}^{-1}\cdot\boldsymbol{F}.$$

Implementing the transformations (25), (26) and (27) in (23) and (24) and taking into account the displacement continuity conditions yields the average strain inside the fiber and the coating,

$$\boldsymbol{\varepsilon}_1 = \frac{1}{2}\left[U_r^{(1)}(r_1) + U_\theta^{(1)}(r_1)\right]\boldsymbol{\varepsilon}_0 \quad \rightarrow \quad \boldsymbol{\varepsilon}_1 = \left[\frac{3K_1^{\rm tr}}{4K_1^{\rm tr}+2\mu_1^{\rm tr}}\Xi_1^{(1)} + \Xi_2^{(1)}\right]\boldsymbol{\varepsilon}_0,$$

$$\boldsymbol{\varepsilon}_2 = \left[\frac{1}{2[1-\rho^2]}\left[U_r^{(0)}(r_2) + U_\theta^{(0)}(r_2)\right] - \frac{\rho^2}{2[1-\rho^2]}\left[U_r^{(1)}(r_1) + U_\theta^{(1)}(r_1)\right]\right]\boldsymbol{\varepsilon}_0 \quad \rightarrow$$

$$\boldsymbol{\varepsilon}_2 = \frac{1}{1-\rho^2}\left[1 + \rho^2\frac{K_0^{\rm tr}+2\mu_0^{\rm tr}}{2\mu_0^{\rm tr}}\Xi_4^{(0)} - \rho^2\frac{3K_1^{\rm tr}}{4K_1^{\rm tr}+2\mu_1^{\rm tr}}\Xi_1^{(1)} - \rho^2\Xi_2^{(1)}\right]\boldsymbol{\varepsilon}_0.$$

Comparing these results with the expressions (22) and (28) it becomes clear that

$$\begin{aligned} T_{1_{44}}^{mm} &= \frac{3K_1^{\rm tr}}{4K_1^{\rm tr}+2\mu_1^{\rm tr}}\Xi_1^{(1)} + \Xi_2^{(1)}, \\ T_{2_{44}}^{mm} &= \frac{1}{1-\rho^2}\left[1 + \rho^2\frac{K_0^{\rm tr}+2\mu_0^{\rm tr}}{2\mu_0^{\rm tr}}\Xi_4^{(0)} - \rho^2\frac{3K_1^{\rm tr}}{4K_1^{\rm tr}+2\mu_1^{\rm tr}}\Xi_1^{(1)} - \rho^2\Xi_2^{(1)}\right]. \end{aligned} \tag{51}$$

4.3. Plane strain and axial electric field conditions

Similarly to the corresponding boundary value problem of the previous section, the infinite matrix is subjected to the far field displacement vector and electric potential of (37). For all phases (matrix, fiber, coating) the general expressions (38) introduce 6 unknowns (2 constants per phase). After eliminating two from the boundary conditions (39), the rest of the unknowns are identified from the interface conditions that hold between the fiber and the coating and between the coating and the matrix. The produced system of linear equations take the form

$$\boldsymbol{K}\cdot\boldsymbol{\Xi} = \boldsymbol{F}_\beta + \frac{\gamma}{\beta}\,\boldsymbol{F}_\gamma,$$

with

$$\begin{aligned}
\boldsymbol{K} &= \begin{bmatrix} 1 & -1 & -1 & 0 \\ 0 & 1 & \rho^2 & -\rho^2 \\ 2K_1^{\mathrm{tr}} & -2K_2^{\mathrm{tr}} & 2\mu_2^{\mathrm{tr}} & 0 \\ 0 & 2K_2^{\mathrm{tr}} & -2\rho^2\mu_2^{\mathrm{tr}} & 2\rho^2\mu_0^{\mathrm{tr}} \end{bmatrix}, \\
\boldsymbol{\Xi} &= \begin{bmatrix} \Xi_1^{(1)} & \Xi_1^{(2)} & \Xi_2^{(2)} & \Xi_2^{(0)} \end{bmatrix}^T, \quad \boldsymbol{F}_\beta = \begin{bmatrix} 0 & 1 & 0 & 2K_0^{\mathrm{tr}} \end{bmatrix}^T, \\
\boldsymbol{F}_\gamma &= \begin{bmatrix} 0 & 0 & e_{1_{31}} - e_{2_{31}} & e_{2_{31}} - e_{0_{31}} \end{bmatrix}^T.
\end{aligned}$$

The solution of this linear system is expressed as

$$\boldsymbol{\Xi} = \boldsymbol{K}^{-1}\cdot\boldsymbol{F}_\beta + \frac{\gamma}{\beta}\boldsymbol{K}^{-1}\cdot\boldsymbol{F}_\gamma.$$

Considering the dilute tensors, the important terms $\Xi_1^{(1)}$ and $\Xi_2^{(0)}$ can be written in the general form

$$\Xi_1^{(1)} = B_1 + \frac{\gamma}{\beta}\,B_2, \quad \Xi_2^{(0)} = B_3 + \frac{\gamma}{\beta}\,B_4.$$

Implementing the transformations (25), (26) and (27) in (23) and (24) and taking into account the displacement continuity conditions yields the average strain inside the fiber and the coating,

$$\begin{aligned}
\boldsymbol{\varepsilon}_1 &= U_r^{(1)}(r_1)\,\boldsymbol{\varepsilon}_0 = B_1 \begin{bmatrix} \beta & 0 & 0 \\ 0 & \beta & 0 \\ 0 & 0 & 0 \end{bmatrix} + B_2 \begin{bmatrix} \gamma & 0 & 0 \\ 0 & \gamma & 0 \\ 0 & 0 & 0 \end{bmatrix}, \\
\boldsymbol{\varepsilon}_2 &= \left[\frac{1}{1-\rho^2} U_r^{(0)}(r_2) - \frac{\rho^2}{1-\rho^2} U_r^{(1)}(r_1) \right] \boldsymbol{\varepsilon}_0 \\
&= \frac{1+\rho^2 B_3 - \rho^2 B_1}{1-\rho^2} \begin{bmatrix} \beta & 0 & 0 \\ 0 & \beta & 0 \\ 0 & 0 & 0 \end{bmatrix} + \frac{\rho^2 B_4 - \rho^2 B_2}{1-\rho^2} \begin{bmatrix} \gamma & 0 & 0 \\ 0 & \gamma & 0 \\ 0 & 0 & 0 \end{bmatrix}.
\end{aligned}$$

The expressions of the dilute concentration tensors (22) and (28) permit to write

$$\varepsilon_{1_{xx}} = [2T_{1_{11}}^{mm} - T_{1_{44}}^{mm}]\,\beta + T_{1_{31}}^{me}\,\gamma, \quad \varepsilon_{2_{xx}} = [2T_{2_{11}}^{mm} - T_{2_{44}}^{mm}]\,\beta + T_{2_{31}}^{me}\,\gamma.$$

From these results it becomes clear that

$$T_{1_{11}}^{mm} = \frac{1}{2}B_1 + \frac{1}{2}T_{1_{44}}^{mm}, \quad T_{1_{31}}^{me} = B_2, \quad T_{2_{11}}^{mm} = \frac{1+\rho^2 B_3 - \rho^2 B_1}{2[1-\rho^2]} + \frac{1}{2}T_{2_{44}}^{mm}, \quad T_{2_{31}}^{me} = \frac{\rho^2 B_4 - \rho^2 B_2}{1-\rho^2}. \tag{52}$$

4.4. Hydrostatic strain conditions

For the remaining terms of the dilute mechanical concentration tensors, the infinite matrix is subjected to the far field displacement vector (43). For all phases (matrix, fiber, coating) the general expressions (44) introduce 6 unknowns (2 constants per phase). After eliminating two from the boundary conditions (45), the rest of the unknowns are identified from the interface conditions that hold between the fiber and the coating and between the coating and the matrix. The produced system of linear equations take the form

$$\boldsymbol{K} \cdot \boldsymbol{\Xi} = \boldsymbol{F},$$

with

$$\boldsymbol{K} = \begin{bmatrix} 1 & -1 & -1 & 0 \\ 0 & 1 & \rho^2 & -\rho^2 \\ 2K_1^{\mathrm{tr}} & -2K_2^{\mathrm{tr}} & 2\mu_2^{\mathrm{tr}} & 0 \\ 0 & 2K_2^{\mathrm{tr}} & -2\rho^2\mu_2^{\mathrm{tr}} & 2\rho^2\mu_0^{\mathrm{tr}} \end{bmatrix},$$

$$\boldsymbol{\Xi} = \begin{bmatrix} \Xi_1^{(1)} & \Xi_1^{(2)} & \Xi_2^{(2)} & \Xi_2^{(0)} \end{bmatrix}^T, \quad \boldsymbol{F} = \begin{bmatrix} 0 & 1 & l_2 - l_1 & 2K_0^{\mathrm{tr}} + l_0 - l_2 \end{bmatrix}^T.$$

The solution of this linear system is expressed as

$$\boldsymbol{\Xi} = \boldsymbol{K}^{-1} \cdot \boldsymbol{F}.$$

Implementing the transformations (25), (26) and (27) in (23) and (24) and taking into account the displacement continuity conditions yields the average strain inside the fiber and the coating,

$$\begin{aligned} \boldsymbol{\varepsilon}_1 &= U_r^{(1)}(r_1)\,\boldsymbol{\varepsilon}_0 = \Xi_1^{(1)}\,\boldsymbol{\varepsilon}_0, \\ \boldsymbol{\varepsilon}_2 &= \left[\frac{1}{1-\rho^2}U_r^{(0)}(r_2) - \frac{\rho^2}{1-\rho^2}U_r^{(1)}(r_1)\right]\boldsymbol{\varepsilon}_0 = \frac{1+\rho^2\Xi_2^{(0)} - \rho^2\Xi_1^{(1)}}{1-\rho^2}\,\boldsymbol{\varepsilon}_0. \end{aligned}$$

The general form of the dilute concentration tensors (22) and (28) permits to write

$$\varepsilon_{1_{xx}} = [2T_{1_{11}}^{mm} - T_{1_{44}}^{mm} + T_{1_{13}}^{mm}]\,\beta, \quad \varepsilon_{2_{xx}} = [2T_{2_{11}}^{mm} - T_{2_{44}}^{mm} + T_{2_{13}}^{mm}]\,\beta.$$

From these results it becomes clear that

$$T_{1_{13}}^{mm} = \Xi_1^{(1)} - 2T_{1_{11}}^{mm} + T_{1_{44}}^{mm}, \qquad T_{2_{13}}^{mm} = \frac{1+\rho^2\Xi_2^{(0)} - \rho^2\Xi_1^{(1)}}{1-\rho^2} - 2T_{2_{11}}^{mm} + T_{2_{44}}^{mm}. \tag{53}$$

The dilute concentration tensors (28), whose terms are given by (50), (51), (52) and (53), can be directly utilized in the Mori-Tanaka scheme, described in subsection 2.2.

5. Numerical examples

To illustrate the capabilities of the proposed methodology, several numerical studies are performed. In the following examples the matrix phase is considered a non-piezoelectric epoxy, the

fibers are PZT-7A and the coating layers (if they exist) are made of PZT-5. The piezoelectric properties for these materials are taken from Berger et al. (2005, 2006) and they are summarized in Table 1.

In the first example, no coating phase is considered. Several macroscopic piezoelectric properties of the fiber composite as a function of the fibers volume fraction are illustrated in Figure 5. In the same plots the numerical results of Berger et al. (2006), which solve periodic unit cell problems with hexagonal arrangement of the fibers through finite element calculations, are utilized as reference values. As shown in the Figure, except from a slight under-prediction in the transverse shear modulus at high fiber content (above 50% volume fraction), the analytical method provides excellent accuracy in identifying the macroscopic response of the composite. As expected, the absolute values of the electromechanical properties show significant increase, almost exponential, at above 50% fiber volume fraction.

	material parameters									
material	n	l	K^{tr}	μ^{tr}	μ^{ax}	e_{31}	e_{33}	e_{15}	κ_{11}	κ_{33}
epoxy	8	4.4	6.2	1.8	1.8	0	0	0	0.0372	0.0372
PZT-7A	131.39	82.712	119.037	35.8	25.696	-2.12058	9.52183	9.34959	4.065	2.079
PZT-5	111	75.2	98.2	22.8	21.1	-5.4	15.8	12.3	8.11	7.35
units	GPa	GPa	GPa	GPa	GPa	Cm^{-2}	Cm^{-2}	Cm^{-2}	$\mathrm{nCV}^{-1}\mathrm{m}^{-1}$	$\mathrm{nCV}^{-1}\mathrm{m}^{-1}$

Table 1: Material parameters for the matrix (epoxy), the fiber (PZT-7A) and the coating layer (PZT-5). The values for the first two materials are taken from Berger et al. (2006), while for the third material are taken from Berger et al. (2005).

In the second parametric study, the same macroscopic properties are compared with those provided by coated fiber composites. The comparisons consider the same fiber content c, while the coating and the matrix have volume fractions that depend on the radii ratio $\rho = r_1/r_2$ between the fiber and the coating/matrix interface, as given by the expressions (49). Since the coating is stronger than the matrix phase, increase in the absolute values of the electromechanical properties is expected for the coated fiber composite. In Figure 6 two coating thicknesses are considered, one with $\rho = 0.95$ and the second with $\rho = 0.90$. In the same Figure, the predictions of the

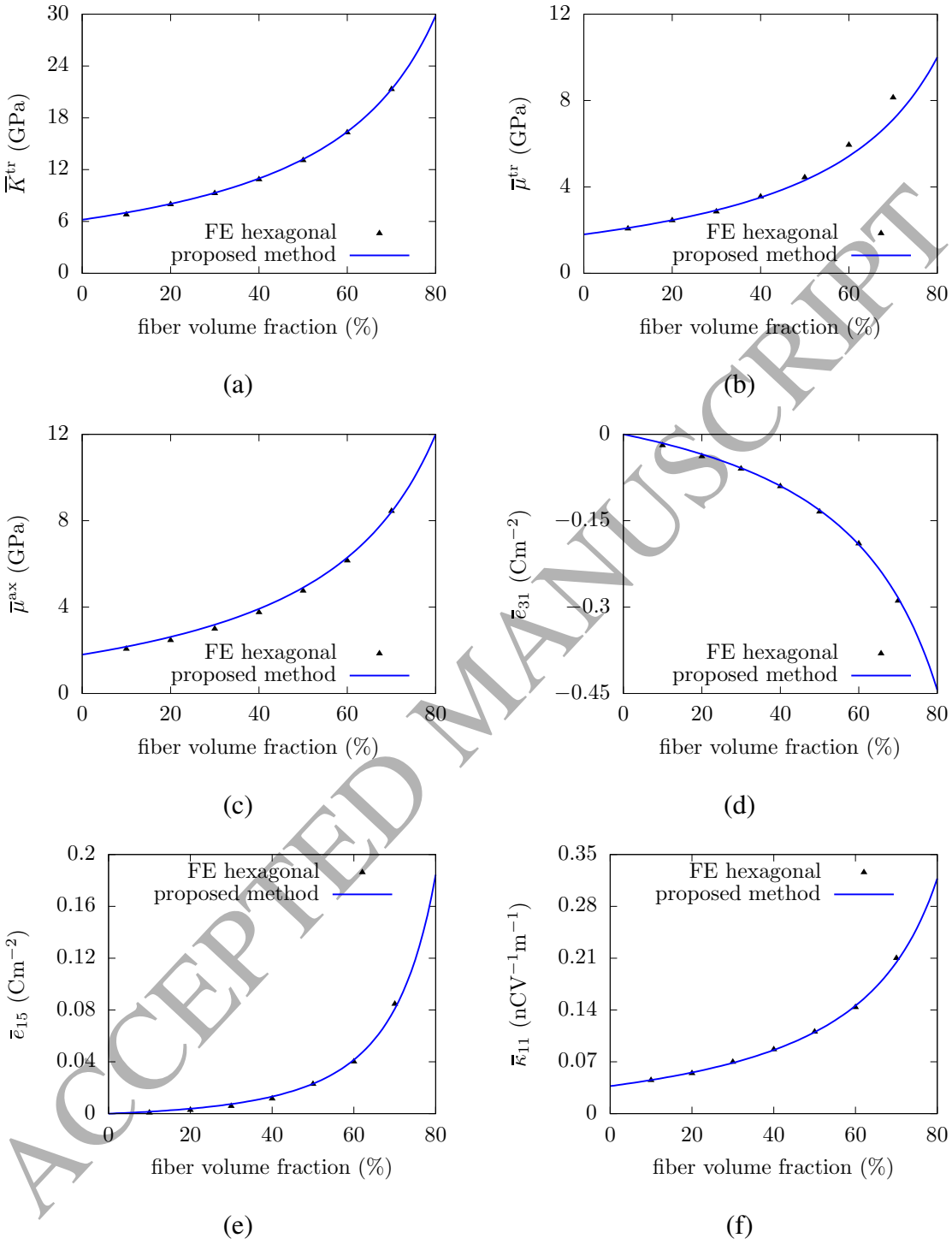

Figure 5: Macroscopic piezoelectric properties of fiber composites without coating: (a) $\overline{K}^{\mathrm{tr}}$, (b) $\overline{\mu}^{\mathrm{tr}}$, (c) $\overline{\mu}^{\mathrm{ax}}$, (d) $\bar{e}_{31}$, (e) $\bar{e}_{15}$ and (f) $\bar{\kappa}_{11}$. Comparison between the proposed method and the numerical results of Berger et al. (2006) using finite element computations in periodic hexagonal unit cells.

proposed method are compared with those obtained by the Mori-Tanaka scheme, when the dilute concentration tensors are obtained through the Koutsawa et al. (2010) framework. Details about this approach are given in Appendix B.

The obtained results show that the coupled piezoelectric parameters are the properties with the highest increase. At 60% fibers volume fraction and $\rho = 0.90$, both $\bar{e}_{31}$ and $\bar{e}_{15}$ become more than 140% higher (in absolute value) compared to the corresponding parameters of the non-coated fiber composite. For the same ρ and fibers volume fraction, the gain in mechanical properties does not exceed 55% and in electrical permittivity does not exceed 66%.

The proposed methodology and the one based on the Mori-Tanaka with the dilute concentration tensors of the Koutsawa et al. (2010) theory (denoted as KBBNC in Figure 6) render exactly the same predictions for all the macroscopic properties, with the exception of the transverse shear modulus. For the $\bar{\mu}^{\text{tr}}$ there is an insignificant difference (less than 0.1%), which is due to the assumption made by Koutsawa et al. (2010) in the usage of the iterfacial operators (see equation (B.7) and the discussion in Appendix B). It is worth mentioning that, in the case of multiple coatings, such assumption affects all the macroscopic properties and it can cumulate a non-negligible error in the macroscopic response. On the other hand, the methodology proposed in this work does not suffer from this issue, since the Eshelby's inhomogeneity problem is solved analytically and the dilute concentration tensors are computed through exact averaging.

As already mentioned in the previous sections, the main advantage of identifying dilute concentration tensors is that they provide information about the average microscopic fields of the various phases, when the macroscopic strain and electric field are known. To demonstrate this capability, it is considered that at a coated fiber composite with fibers volume fraction 45% and

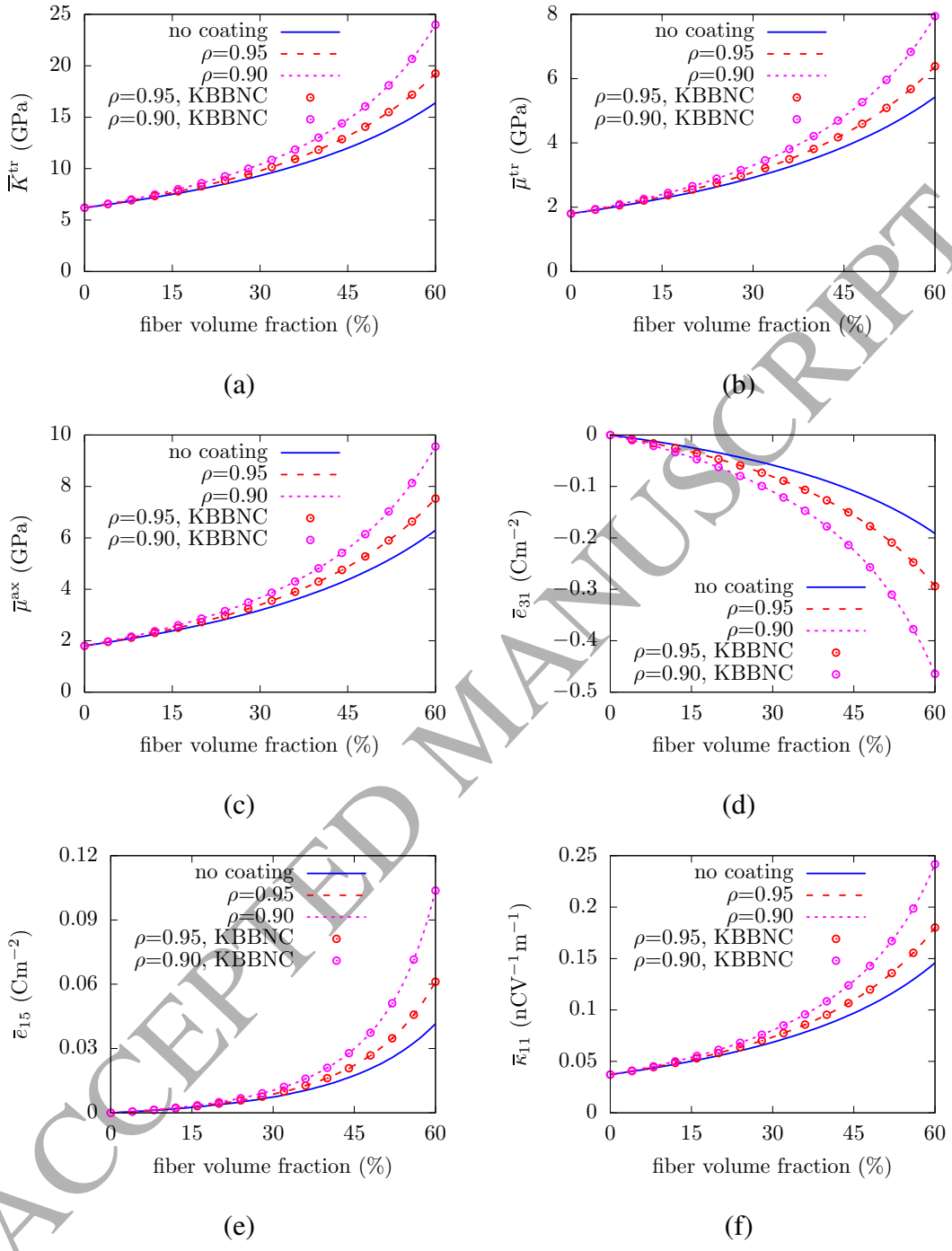

Figure 6: Macroscopic piezoelectric properties of fiber composites: (a) $\bar{K}^{tr}$, (b) $\bar{\mu}^{tr}$, (c) $\bar{\mu}^{ax}$, (d) $\bar{e}_{31}$, (e) $\bar{e}_{15}$ and (f) $\bar{\kappa}_{11}$. Comparison between non-coated fibers and coated fibers with $\rho = 0.95$ and $\rho = 0.90$. The dashed lines correspond to the prediction of the current methodology and the points to the predictions of the Mori-Tanaka scheme with the dilute concentration tensors according to the Koutsawa et al. (2010) theory.

$\rho = 0.9$, the following uniform macroscopic strain tensor and electric field vector are applied:

$$\bar{\boldsymbol{\varepsilon}} = \begin{bmatrix} \bar{\varepsilon}_{xx} \\ \bar{\varepsilon}_{yy} \\ \bar{\varepsilon}_{zz} \\ 2\bar{\varepsilon}_{xy} \\ 2\bar{\varepsilon}_{xz} \\ 2\bar{\varepsilon}_{yz} \end{bmatrix} = \begin{bmatrix} 7 \\ 6 \\ 8 \\ 2 \\ 4 \\ 6 \end{bmatrix} \cdot 10^{-4}, \quad \bar{\boldsymbol{E}} = \begin{bmatrix} \bar{E}_x \\ \bar{E}_y \\ \bar{E}_z \end{bmatrix} = \begin{bmatrix} 1 \\ 2 \\ 1 \end{bmatrix} \cdot 10^{-4} \frac{\mathrm{GV}}{\mathrm{m}}.$$

For these macroscopic conditions, the average microscopic fields at all phases (matrix, fiber, coating), as well as the macroscopic stresses and electric displacements are summarized in Table 2.

6. Conclusions

The article presented a micromechanical approach for identifying dilute concentration tensors for piezoelectric multi-coated, long fiber composites, which can be utilized in classical homogenization schemes, such as Mori-Tanaka and self consistent. The procedure shown here for non-coated and coated fibers with one layer is applicable to fibers with multiple coating layers, by using the boundary value problems and the analytical formalism described in sections 3 and 4. The extensive comparisons with known analytical and computational results from the literature illustrated the method's reliability and capabilities.

The main advantage of the proposed methodology is that it solves analytically the Eshelby's inhomogeneity problem, which in turn permits the exact computation of the dilute concentration piezoelectric tensors. The described procedure is also easily extendable to account for other types of mechanisms, like thermomechanical behavior or inelastic response through a transformation field analysis type approach. In addition, the proposed approach provides new capabilities in studying piezoelectric composite materials and permits, with proper modifications, to account for imperfect mechanical (Chatzigeorgiou et al., 2017) and/or dielectric (Chatzigeorgiou et al., 2015) interfaces between the material constituents.

component	macroscopic	matrix	fiber	coating	units
ε_{xx}	$7\cdot10^{-4}$	$1.7531\cdot10^{-3}$	$-1.4265\cdot10^{-4}$	$-1.4171\cdot10^{-4}$	-
ε_{yy}	$6\cdot10^{-4}$	$1.5502\cdot10^{-3}$	$-1.5904\cdot10^{-4}$	$-1.6497\cdot10^{-4}$	-
ε_{zz}	$8\cdot10^{-4}$	$8\cdot10^{-4}$	$8\cdot10^{-4}$	$8\cdot10^{-4}$	-
$2\varepsilon_{xy}$	$2\cdot10^{-4}$	$4.0576\cdot10^{-4}$	$3.2781\cdot10^{-5}$	$4.6524\cdot10^{-5}$	-
$2\varepsilon_{xz}$	$4\cdot10^{-4}$	$8.1990\cdot10^{-4}$	$6.3082\cdot10^{-5}$	$6.8347\cdot10^{-5}$	-
$2\varepsilon_{yz}$	$6\cdot10^{-4}$	$1.2294\cdot10^{-3}$	$9.4964\cdot10^{-5}$	$1.0282\cdot10^{-4}$	-
σ_{xx}	28.0887	24.3656	31.0563	31.1138	MPa
σ_{yy}	27.1241	23.6353	29.8827	30.0531	MPa
σ_{zz}	51.7193	20.9345	79.2065	64.1572	MPa
σ_{xy}	0.9647	0.7304	1.1736	1.0608	MPa
σ_{xz}	2.2316	1.4758	2.8276	2.8731	MPa
σ_{yz}	3.3459	2.2130	4.2398	4.3056	MPa
E_x	$1\cdot10^{-4}$	$3.8331\cdot10^{-4}$	$-1.2906\cdot10^{-4}$	$-1.1634\cdot10^{-4}$	GV/m
E_y	$2\cdot10^{-4}$	$6.8614\cdot10^{-4}$	$-1.9248\cdot10^{-4}$	$-1.7367\cdot10^{-4}$	GV/m
E_z	$1\cdot10^{-4}$	$1\cdot10^{-4}$	$1\cdot10^{-4}$	$1\cdot10^{-4}$	GV/m
D_x	$2.4798\cdot10^{-5}$	$1.4259\cdot10^{-5}$	$6.5144\cdot10^{-5}$	$-1.0283\cdot10^{-4}$	C/m^2
D_y	$4.3609\cdot10^{-5}$	$2.5524\cdot10^{-5}$	$1.0543\cdot10^{-4}$	$-1.4378\cdot10^{-4}$	C/m^2
D_z	$5.3976\cdot10^{-3}$	$3.7200\cdot10^{-6}$	$8.4651\cdot10^{-3}$	$1.5031\cdot10^{-2}$	C/m^2

Table 2: Macroscopic and average microscopic fields in a coated fiber composite with fibers volume fraction 45% and $\rho = 0.9$.

Appendix A. Eshelby tensor for infinitely long cylinder in piezoelectric material

In a piezoelectric material, the constitutive law equations (1) can be expressed in the global matrix form

$$\boldsymbol{\Sigma} = \boldsymbol{L} \cdot \boldsymbol{Z}, \tag{A.1}$$

where $\boldsymbol{\Sigma}$ and $\boldsymbol{Z}$ are the stress/electric displacement and strain/electric field tensors respectively, written as 9×1 vectors

$$\begin{aligned} \boldsymbol{\Sigma} &= \begin{bmatrix} \boldsymbol{\sigma} \\ \boldsymbol{D} \end{bmatrix} = \begin{bmatrix} \sigma_{xx} & \sigma_{yy} & \sigma_{zz} & 2\sigma_{xy} & 2\sigma_{xz} & 2\sigma_{yz} & D_x & D_y & D_z \end{bmatrix}^T, \\ \boldsymbol{Z} &= \begin{bmatrix} \boldsymbol{\varepsilon} \\ -\boldsymbol{E} \end{bmatrix} = \begin{bmatrix} \varepsilon_{xx} & \varepsilon_{yy} & \varepsilon_{zz} & 2\varepsilon_{xy} & 2\varepsilon_{xz} & 2\varepsilon_{yz} & -E_x & -E_y & -E_z \end{bmatrix}^T, \end{aligned} \tag{A.2}$$

and $\boldsymbol{L}$ is the symmetric global piezoelectric tensor, written as 9×9 matrix

$$\boldsymbol{L} = \begin{bmatrix} \boldsymbol{C} & \boldsymbol{e} \\ \boldsymbol{e}^T & -\boldsymbol{\kappa} \end{bmatrix}. \tag{A.3}$$

Dunn and Taya (1993) have obtained analytical expressions for the Eshelby tensor, $\boldsymbol{S}$, considering a transversely isotropic piezoelectric material, written in the grobal form (A.1), and infinitely

long cylindrical fiber. In Voigt notation, $\boldsymbol{S}$ is expressed as

$$\boldsymbol{S} = \begin{bmatrix} \frac{3K^{\mathrm{tr}}+2\mu^{\mathrm{tr}}}{4K^{\mathrm{tr}}+4\mu^{\mathrm{tr}}} & \frac{K^{\mathrm{tr}}-2\mu^{\mathrm{tr}}}{4K^{\mathrm{tr}}+4\mu^{\mathrm{tr}}} & \frac{l}{2K^{\mathrm{tr}}+2\mu^{\mathrm{tr}}} & 0 & 0 & 0 & 0 & \frac{e_{31}}{2K^{\mathrm{tr}}+2\mu^{\mathrm{tr}}} \\ \frac{K^{\mathrm{tr}}-2\mu^{\mathrm{tr}}}{4K^{\mathrm{tr}}+4\mu^{\mathrm{tr}}} & \frac{3K^{\mathrm{tr}}+2\mu^{\mathrm{tr}}}{4K^{\mathrm{tr}}+4\mu^{\mathrm{tr}}} & \frac{l}{2K^{\mathrm{tr}}+2\mu^{\mathrm{tr}}} & 0 & 0 & 0 & 0 & \frac{e_{31}}{2K^{\mathrm{tr}}+2\mu^{\mathrm{tr}}} \\ 0 & 0 & 0 & 0 & 0 & 0 & 0 & 0 \\ 0 & 0 & 0 & \frac{K^{\mathrm{tr}}+2\mu^{\mathrm{tr}}}{2K^{\mathrm{tr}}+2\mu^{\mathrm{tr}}} & 0 & 0 & 0 & 0 \\ 0 & 0 & 0 & 0 & \frac{1}{2} & 0 & 0 & 0 \\ 0 & 0 & 0 & 0 & 0 & \frac{1}{2} & 0 & 0 \\ 0 & 0 & 0 & 0 & 0 & 0 & \frac{1}{2} & 0 \\ 0 & 0 & 0 & 0 & 0 & 0 & 0 & \frac{1}{2} \\ 0 & 0 & 0 & 0 & 0 & 0 & 0 & 0 \end{bmatrix}. \quad \text{(A.4)}$$

Considering a fiber with piezoelectric properties $\boldsymbol{L}_1$, the dilute concentration tensor of the combined electromechanical problem is connected with the above Eshelby tensor through the classical relation

$$\boldsymbol{T} = \left[\mathbb{I} + \boldsymbol{S}\colon\boldsymbol{L}^{-1}\colon[\boldsymbol{L}_1 - \boldsymbol{L}]\right]^{-1}, \quad \text{(A.5)}$$

where $\mathbb{I}$ is the extended identity tensor, which in Voigt notation is written as the 9×9 identity matrix. Substituting $\boldsymbol{L}$ with $\boldsymbol{L}_0$ and accounting for the negative sign of the electric field, renders a $\boldsymbol{T}$ that is equivalent to the system of the four dilute concentration tensors obtained in section 3.

Appendix B. Dilute concentration tensors based on the Koutsawa et al. (2010) theory

For a composite with multi-coated ellipsodal shape particles, Koutsawa et al. (2010) have identified global thermo-electro-elastic concentration tensors of all phases for the self consistent method and have obtained the macroscopic thermo-electro-elastic properties. When considering the Mori-Tanaka method, these global concentration tensors can be translated to dilute concentration tensors, if one substitutes the effective medium with the matrix (Chatzigeorgiou et al., 2018). This Appendix presents the essential points of the Koutsawa et al. (2010) approach for obtaining dilute piezoelectric concentration tensors for a coated, infinitely long fiber with a single coating layer.

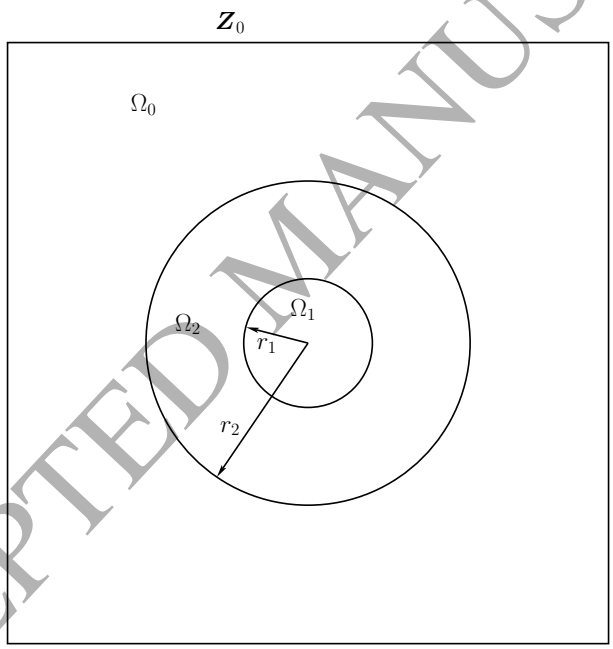

Figure B.1: Coated fiber with a single coating layer inside a matrix, subjected to uniform strain and electric field at far distance. All phases are piezoelectric materials.

The Eshelby inhomogeneity problem considers a piezoelectric coated fiber embedded inside the linear piezoelectric matrix, (Figure B.1). The fiber occupies the space Ω_1 with volume V_1, its coating the space Ω_2 with volume V_2, and the matrix occupies the space Ω_0, which is extended to far distance from the fiber. Adopting the notation of Appendix A for the combined electromechan-

ical constitutive response, the matrix is subjected to uniform strain/electric field extended vector $\boldsymbol{Z}_0$ at the far field. The interface between each phase is considered perfect. The ratio between the fiber radius r_1 and the external radius of the interface r_2 is denoted as $\rho = r_1/r_2$. The matrix is characterized by the piezoelectic tensor $\boldsymbol{L}_0$, the fiber by the tensor $\boldsymbol{L}_1$ and the coating by the tensor $\boldsymbol{L}_2$.

The piezoelectric properties in this Eshelby problem vary spatially and can be expressed in the differential form

$$\boldsymbol{L}(\boldsymbol{x}) = \boldsymbol{L}_0 + \delta\boldsymbol{L}(\boldsymbol{x}), \qquad \boldsymbol{x} \in \Omega, \tag{B.1}$$

where Ω denotes the total space $\Omega = \Omega_0 \cup \Omega_1 \cup \Omega_2$ and $\delta\boldsymbol{L}(\boldsymbol{x})$ denotes spatial alteration of the matrix properties at the region of the coating and of the fiber:

$$\begin{gathered}\delta\boldsymbol{L}(\boldsymbol{x}) = [\boldsymbol{L}_1 - \boldsymbol{L}_0]\,\theta_1(\boldsymbol{x}) + [\boldsymbol{L}_2 - \boldsymbol{L}_0]\,\theta_2(\boldsymbol{x}), \\ \theta_1(\boldsymbol{x}) = \begin{cases} 1 & \forall \boldsymbol{x} \in \Omega_1 \\ 0 & \forall \boldsymbol{x} \notin \Omega_1 \end{cases}, \quad \theta_2(\boldsymbol{x}) = \begin{cases} 1 & \forall \boldsymbol{x} \in \Omega_2 \\ 0 & \forall \boldsymbol{x} \notin \Omega_2 \end{cases}.\end{gathered} \tag{B.2}$$

Employing Green's formalism, the simplified equation for the $\boldsymbol{Z}$ vector at any point is written (Korringa, 1973; Zeller and Dederichs, 1973)

$$\boldsymbol{Z}(\boldsymbol{x}) = \boldsymbol{Z}_0 - \int_\Omega \boldsymbol{\Gamma}^0(\boldsymbol{x} - \boldsymbol{x}') : \delta\boldsymbol{L}(\boldsymbol{x}') : \boldsymbol{Z}(\boldsymbol{x}')\mathrm{d}\boldsymbol{x}', \tag{B.3}$$

where $\Gamma^0(\boldsymbol{x} - \boldsymbol{x}')$ is the piezoelectric modified Green's tensor. Averaging over the space $\Omega_1 \cup \Omega_2$ of the fiber/coating system yields (Koutsawa et al., 2010)

$$\boldsymbol{Z}_c = \boldsymbol{Z}_0 - \rho^2\, \boldsymbol{S}(\boldsymbol{L}_0) : \boldsymbol{L}_0^{-1} : [\boldsymbol{L}_1 - \boldsymbol{L}_0] : \boldsymbol{Z}_1 - [1 - \rho^2]\, \boldsymbol{S}(\boldsymbol{L}_0) : \boldsymbol{L}_0^{-1} : [\boldsymbol{L}_2 - \boldsymbol{L}_0] : \boldsymbol{Z}_2. \tag{B.4}$$

In the above expression, $\boldsymbol{Z}_1$, $\boldsymbol{Z}_2$ and $\boldsymbol{Z}_c$ are the average $\boldsymbol{Z}$ tensors in the fiber, the coating and the fiber/coating combined system respectively, connected with the relation

$$\boldsymbol{Z}_c = \rho^2\, \boldsymbol{Z}_1 + [1 - \rho^2]\, \boldsymbol{Z}_2, \tag{B.5}$$

while $\boldsymbol{S}(\boldsymbol{L}_0)$ denotes the extended Eshelby tensor that depends on the matrix properties and the shape of the coated fiber system, which is infinitely long cylinder. Appendix A gives the analytical form of this tensor for transversely isotropic material response. The connection between the

average $\boldsymbol{Z}$ tensors in the fiber and the coating is given with the help of Hill's interfacial operators. The jump of $\boldsymbol{Z}$ across an interface between two materials is given by

$$\boldsymbol{Z}^{+}(\boldsymbol{x}) = [\mathbb{I} + \boldsymbol{P}(\boldsymbol{L}_2)\colon [\boldsymbol{L}_1 - \boldsymbol{L}_2]] : \boldsymbol{Z}^{-}, \tag{B.6}$$

where $\mathbb{I}$ is the extended identity tensor and $\boldsymbol{P}(\boldsymbol{L}_2)$ is the interfacial operator, which depends on the coating properties. At this point, the main approximation is that the $\boldsymbol{Z}^{-}$ is substituted with the average value $\boldsymbol{Z}_1$ in the fiber. With this assumption, accounting for the homothetic topology of the fiber and the coating and averaging (B.6) over the space Ω_2 yields

$$\boldsymbol{Z}_2 = \left[\mathbb{I} + \boldsymbol{S}(\boldsymbol{L}_2)\colon \boldsymbol{L}_2^{-1}\colon [\boldsymbol{L}_1 - \boldsymbol{L}_2]\right] : \boldsymbol{Z}_1. \tag{B.7}$$

$\boldsymbol{S}(\boldsymbol{L}_2)$ denotes the extended Eshelby tensor, which is a function of the coating piezoelectric tensor and the shape of the fiber. For multiple coating layers, equations similar to the last one connect the strain/electric field combined vectors between two consequent layers.

Expression (B.7) is exact only when the strain and the electric field inside the fiber is uniform. For single layer coated fibers, the four boundary value problems of section 4 show that only the case of transverse shear renders non-uniform strain inside the fiber: the term $\Xi_1^{(1)}$ of equation (51) is generally non-zero, and thus the shear strain inside the fiber depends quadratically on the radial distance. As demonstrated in section 5, this non-uniformity has a practically insignificant effect in the macroscopic transverse shear modulus.

Combining (B.4), (B.5) and (B.7) and after some algebra, one obtains

$$\begin{aligned} \boldsymbol{Z}_1 &= \boldsymbol{T}_1 \colon \boldsymbol{Z}_0, \qquad & \boldsymbol{Z}_2 &= \boldsymbol{T}_2 \colon \boldsymbol{Z}_0, \\ \boldsymbol{T}_1 &= \left[\rho^2\, \boldsymbol{N}_{10} + [1-\rho^2]\;\; \boldsymbol{N}_{20} \colon \boldsymbol{N}_{12}\right]^{-1}, \qquad & \boldsymbol{T}_2 &= \boldsymbol{N}_{12} \colon \boldsymbol{T}_1, \end{aligned} \tag{B.8}$$

with

$$\begin{aligned} \boldsymbol{N}_{10} &= \mathbb{I} + \boldsymbol{S}(\boldsymbol{L}_0) \colon \boldsymbol{L}_0^{-1} \colon [\boldsymbol{L}_1 - \boldsymbol{L}_0]\,, \\ \boldsymbol{N}_{20} &= \mathbb{I} + \boldsymbol{S}(\boldsymbol{L}_0) \colon \boldsymbol{L}_0^{-1} \colon [\boldsymbol{L}_2 - \boldsymbol{L}_0]\,, \\ \boldsymbol{N}_{12} &= \mathbb{I} + \boldsymbol{S}(\boldsymbol{L}_2) \colon \boldsymbol{L}_2^{-1} \colon [\boldsymbol{L}_1 - \boldsymbol{L}_2]\,. \end{aligned} \tag{B.9}$$

The tensors $\boldsymbol{T}_1$ and $\boldsymbol{T}_2$ are the required dilute concentration tensors that can be integrated into the Mori-Tanaka micromechanical scheme.

The Mori-Tanaka in this formalism follows the usual procedure for three phase composite: considering a coated fiber composite with c_0, c_1 and c_2 the volume fractions of the matrix, the fiber and the coating respectively (see equations (49)), the global concentration tensors for all phases are written as

$$\boldsymbol{A}_0 = [c_0\mathbb{I} + c_1\boldsymbol{T}_1 + c_2\boldsymbol{T}_2]^{-1}, \qquad \boldsymbol{A}_1 = \boldsymbol{T}_1 : \boldsymbol{A}_0, \qquad \boldsymbol{A}_2 = \boldsymbol{T}_2 : \boldsymbol{A}_0. \tag{B.10}$$

The macroscopic combined piezoelectric tensor $\bar{\boldsymbol{L}}$ of the coated fiber composite is then given by the expression

$$\bar{\boldsymbol{L}} = c_0\boldsymbol{L}_0 : \boldsymbol{A}_0 + c_1\boldsymbol{L}_1 : \boldsymbol{A}_1 + c_2\boldsymbol{L}_2 : \boldsymbol{A}_2. \tag{B.11}$$

References

References

Aboudi, J., 2001. Micromechanical analysis of fully coupled electro-magneto-thermo-elastic multiphase composites. Smart Materials and Structures 10, 867–877.

Benveniste, Y., 1994. On the micromechanics of fibrous piezoelectric composites. Mechanics of Materials 18, 183–193.

Benveniste, Y., Dvorak, G. J., 1992. Uniform fields and universal relations in piezoelectric composites. Journal of the Mechanics and Physics of Solids 40, 1295–1312.

Benveniste, Y., Dvorak, G. J., Chen, T., 1989. Stress fields in composites with coated inclusions. Mechanics of Materials 7, 305–317.

Benveniste, Y., Dvorak, G. J., Chen, T., 1991. On diagonal and elastic symmetry of the approximate effective stiffness tensor oh heterogeneous media. Journal of the Mechanics and Physics of Solids 39 (7), 927–946.

Berger, H., Kari, S., Gabbert, U., Rodriguez-Ramos, R., Bravo-Castillero, J., Guinovart-Diaz, R., Sabina, F. G., Maugin, G., 2006. Unit cell models of piezoelectric fiber composites for numerical and analytical calculation of effective properties. Smart Materials and Structures 15, 451–458.

Berger, H., Kari, S., Gabbert, U., Rodriguez-Ramos, R., Guinovart, R., Otero, J. A., Bravo-Castillero, J., 2005. An analytical and numerical approach for calculating effective material coefficients of piezoelectric fiber composites. International Journal of Solids and Structures 42, 5692–5714.

Bravo-Castillero, J., Rodríguez-Ramos, R., Mechkour, H., Otero, J. A., Cabanas, J. H., Sixto, L. M., Guinovart-Díaz, R., Sabina, F. J., 2009. Homogenization and effective properties of periodic thermomagnetoelectroelastic composites. Journal of Mechanics of Materials and Structures 4 (5), 819–836.

Chatzigeorgiou, G., Charalambakis, N., Chemisky, Y., Meraghni, F., 2018. Thermomechanical Behavior of Dissipative Composite Materials. ISTE Press - Elsevier, London.

Chatzigeorgiou, G., Javili, A., Steinmann, P., 2015. Interface properties influence the effective dielectric constant of composites. Philosophical Magazine 95 (28-30), 3402–3412.

Chatzigeorgiou, G., Meraghni, F., Javili, A., 2017. Generalized interfacial energy and size effects in composites. Journal of the Mechanics and Physics of Solids 106, 257–282.

Chatzigeorgiou, G., Seidel, G. D., Lagoudas, D. C., 2012. Effective mechanical properties of aligned "fuzzy fiber" composites. Composites Part B: Engineering, special issue "Homogenization and Micromechanics of Smart and Multifunctional Materials" 43, 2577–2593.

Christensen, R. M., Lo, K. H., 1979. Solutions for effective shear properties in three phase sphere and cylinder models. Journal of the Mechanics and Physics of Solids 27, 315–330.

Dunn, M. L., Taya, M., 1993. Micromechanics predictions of the effective electroelastic moduli of piezoelectric composites. International Journal of Solids and Structures 30 (2), 161–175.

Dvorak, G., 1992. Transformation field analysis of inelastic composite materials. Proceedings of the Royal Society of London A 437, 311–327.

Dvorak, G., Benveniste, Y., 1992. On transformation strains and uniform fields in multiphase elastic media. Proceedings of the Royal Society of London A 437, 291–310.

Gu, S. T., He, Q. C., Pensée, V., 2015. Homogenization of fibrous piezoelectric composites with general imperfect interfaces under anti-plane mechanical and in-plane electrical loadings. Mechanics of Materials 88 94, 12–29.

Gu, S. T., Liu, J. T., He, Q. C., 2014. Piezoelectric composites: Imperfect interface models, weak formulations and benchmark problems. Computational Materials Science 94, 182–190.

Hashin, Z., 1990. Thermoelastic properties of fiber composites with imperfect interface. Mechanics of Materials 8, 333–348.

Hashin, Z., Rosen, B. W., 1964. The elastic moduli of fiber-reinforced materials. Journal of Applied Mechanics 31, 223–232.

Hossain, M., Chatzigeorgiou, G., Meraghni, F., Steinmann, P., 2015. A multi-scale approach to model the curing process in magneto-sensitive polymeric materials. International Journal of Solids and Structures 69-70, 34–44.

Kalamkarov, A. L., Kolpakov, A. G., 2001. A new asymptotic model for a composite piezoelastic plate. International Journal of Solids and Structures 38, 6027–6044.

Korringa, J., 1973. Theory of elastic Constants of heterogeneous media. Journal of Mathematical Physics 14, 509–513.

Koutsawa, Y., Biscani, F., Belouettar, S., Nasser, H., Carrera, E., 2010. Multi-coating inhomogeneities approach for the effective thermo-electro-elastic properties of piezoelectric composite materials. Composite Structures 92, 964–972.

Lee, J., Boyd IV, J. G., Lagoudas, D. C., 2005. Effective properties of three-phase electro-magneto-elastic composites.

International Journal of Engineering Science 43, 790–825.

Li, J. Y., Dunn, M. L., 1998. Micromechanics of Magnetoelectroelastic Composite Materials: Average Fields and Effective Behavior. Journal of Intelligent Material Systems and Structures 9, 404–416.

Maruccio, C., De Lorenzis, L., Persano, L., Pisignano, D., 2015. Computational homogenization of fibrous piezoelectric materials. Computational Mechanics 55 (5), 983–998.

Pakam, N., Arockiarajan, A., 2014. Study on effective properties of 1-3-2 type magneto-electro-elastic composites. Sensors and Actuators A: Physical 209, 87–99.

Payandeh, Y., Meraghni, F., Patoor, E., Eberhardt, A., 2010. Debonding initiation in a NiTi shape memory wireepoxy matrix composite. Influence of martensitic transformation. Materials and Design 31, 1077–1084.

Payandeh, Y., Meraghni, F., Patoor, E., Eberhardt, A., 2012. Study of the martensitic transformation in NiTiepoxy smart composite and its effect on the overall behavior. Materials and Design 39, 104–110.

Ray, M. C., Batra, R. C., 2009. Effective Properties of Carbon Nanotube and Piezoelectric Fiber Reinforced Hybrid Smart Composites. Journal of Applied Mechanics 76, 034503.

Seidel, G. D., Chatzigeorgiou, G., Ren, X., Lagoudas, D. C., 2014. Multiscale Modeling of Multifunctional Fuzzy Fibers based on Multi-Walled Carbon Nanotubes. In: Tserpes, K. I., Silvestre, N. P. (Eds.), Modeling of Carbon Nanotubes, Graphene and their Composites. Vol. 188 of Springer Series in Materials Science. Springer International Publishing, Cham, pp. 135–176.

Sharma, N. D., Maranganti, R., Sharma, P., 2007. On the possibility of piezoelectric nanocomposites without using piezoelectric materials. Journal of the Mechanics and Physics of Solids 55, 2328–2350.

Spinelli, S. A., Lopez-Pamies, O., 2014. A general closed-form solution for the overall response of piezoelectric composites with periodic and random particulate microstructures. International Journal of Solids and Structures 51, 2979–2989.

Wang, Z., Oelkers, R. J., Lee, K. C., Fisher, F. T., 2016. Annular Coated Inclusion model and applications for polymer nanocomposites Part II: Cylindrical inclusions. Mechanics of Materials 101, 50–60.

Wang, Z., Zhu, J., Jin, X. Y., Chen, W. Q., Zhang, C., 2014. Effective moduli of ellipsoidal particle reinforced piezoelectric composites with imperfect interfaces. Journal of the Mechanics and Physics of Solids 65, 138–156.

Zeller, R., Dederichs, P. H., 1973. Elastic Constants of Polycrystals. Physica status solidi (b) 55, 831–842.

Zou, W. N., He, Q. C., Zheng, Q. S., 2011. General solution for Eshelbys problem of 2D arbitrarily shaped piezoelectric inclusions. International Journal of Solids and Structures 48, 2681–2694.